Nansen Environmental and Remote Sensing Center

NERSC Technical Report no. 267

Sea ice modelling and remote sensing in the Barents and Kara Sea
Part A: Sea ice modelling

Photograph of an iceberg drifting in sea ice. Courtesy: A. Glazovsky

Project for Statoil ASA in 2005

Statoil Order no. 4500909324

Authors:
*Stein Sandven, Laurent Bertino, Knut Arild Lisæter, Intissar Keghouche, Hanne Sagen,
Kjell Kloster, and Mohamed Babiker*

January 2006

NERSC

Mohn-Sverdrup Center
Global Ocean Studies - Operational Oceanography

TITLE:	REPORT IDENTIFICATION
Sea ice modeling and remote sensing in the Barents and Kara Seas **Part A: Sea ice modelling**	**NERSC Technical report no. 267**

CLIENT	CONTRACT
STATOIL ASA	Order no. 4500909324

CLIENT REFERENCE	AVAILABILITY
Einar Nygaard	Customer report

INVESTIGATORS	AUTHORISATION
Stein Sandven, Laurent Bertino, Knut Arild Lisæter, Intissar Keghouche, Hanne Sagen, Kjell Kloster, and Mohamed Babiker	Bergen, 20 January 2006 Stein Sandven

Contents

Executive Summary

Part A of this report describes the ice-ocean modeling work carried out in the Arctic Ocean and with focus on the Barents Sea & Kara Sea area under the contract between the Nansen Center and Statoil for 2005. The main activity has been to set up and run test simulations with the high resolution coupled sea ice – ocean model with about 5 km resolution (the Barents Sea model). The Barents Sea model is nested with the large-scale TOPAZ system covering the whole North Atlantic and Arctic. Like the TOPAZ system, the Barents Sea model is based on the HYCOM ocean model and uses Elastic Visco Plastic (EVP) rheology for the sea ice model. The atmospheric forcing fields are from European Centre for Medium-Range Weather Forecasts (ECMWF).

The Barents Sea model have been run for four months in 1979, which was a heavy ice year, and validated with respect to water mass fluxes, temperature and salinity fields and ice edge/ice concentration. An iceberg model have been obtained from Alfred Wegener Institute and will be coupled to the Barents Sea model in 2006. From these components an iceberg drift forecasting model will be implemented and validated.

Ice thickness simulations from the North Atlantic model, run for the period 1958 – 2002, have obtained and validated for the Arctic Basin. Ice thickness statistics in selected parts of the Barents Sea have been estimated. The Barents Sea model including the iceberg model will be further tested and validated in 2006. The objective is to establish an operational forecasting system for icebergs, sea ice drift and currents by 2007.

Part B described the satellite remote sensing activities performed in the Statoil contract for 2005. We have collected and analysed several types of satellite data that can quantify some of the sea ice and iceberg properties that are important for planning of Statoil's activities in the Barents and Kara Sea region. Daily passive microwave data are useful for mapping ice concentration and ice extent on regional scale in order to follow the ice edge and ice drift. These parameters are needed as input data in sea ice and iceberg drift models. At present daily, near real-time data are assimilated in the TOPAZ ice forecasting model, and will be used also in the Barents Sea model.

For detailed mapping of ice types, ice concentration, ice drift, ice convergence/divergence, multiyear floes, ridges and leads SAR images have been collected for most of the study period in 2005. Several examples of analysis of the SAR images, including ice drift retrieval, have been shown. From February SAR wideswath mosaics have been made more or less regularly throughout the year in the Barents/Kara Sea region. This demonstrates how ice mapping can be improved compared to the standard ice charts delivered by the national ice services. 2005 is the fist year when such SAR mosaics are produced in the Barents/Kara Sea region. SAR is the most important space instrument for mapping sea ice properties in support of ice operations and navigation.

For iceberg detection, high resolution optical images have been demonstrated in the Franz Josef Land area. In one ASTER image more that 100 icebergs were found embedded in the fastice surrounding the archipelago in May 2005. For monitoring of iceberg production and iceberg drift, it is useful to have a systematic scheme for optical as well as SAR images with sufficient high resolution. Use of satellite altimeter data for ice surface topography, ridges and thickness mapping has been investigated with examples of IceSat data from 2003.

Finally, recommendations for further work are indicated in both part A and B.

1. Introduction to the modeling systems

1.1 Overview of ice-ocean models at NERSC

Several ice-ocean model systems are developed and used at NERSC, see Table 1 for a summary. The operational TOPAZ system (Bertino et al. 2004), the Global ice-ocean model and the North-Atlantic model are run under various EU and national projects, while the high resolution Barents Sea model has been initiated under the EU SITHOS-project which was completed in 2005.

All ice models, except the Global ice-ocean model, use Elastic Visco Plastic (EVP) rheology by Hunke and Dukowicz (1997). The Global ice-ocean model uses viscous-plastic rheology (Hibler III, 1979). A single category ice model is used in TOPAZ, Barents Sea model and the Global ice-ocean model, while a multi category ice model is used in the North-Atlantic model. The Barents Sea model will be upgraded to use multi-category ice model when the nesting routines have been upgraded to incorporate data from multi category models. In the following we describe each of the model systems and examples of results derived from them.

Table 1. Ice-ocean modeling systems at NERSC

Ice-ocean model system	Model components	Ocean resolution & layers	Assimilation	Modelling period	Geographical region
TOPAZ	Ocean: HYCOM Ice: EVP rheology	20-22 km resolution; 22 layers in vertical	EnKF / 100 members	Start : 01.01.2003 Up to real time	Atlantic & Arctic regions
North-Atlantic model	Ocean: HYCOM Ice: EVP rheology, Multi-category ice thickness	40-70 km resolution; 26 layers in vertical	None, Free run, Single member	Start: 01.09.1958 Integrated up to 2002	North Atlantic & Arctic regions
Global ice-ocean model	Ocean: MICOM Ice: Viscous-plastic rheology	40 km resolution; 26 layers in vertical	None, Free run, Single member	Start: 01.01.1948 Current end 01.01.2003	Global
Barents Sea model	Ocean: HYCOM Ice: EVP rheology	5 km resolution; 22 layers	None, Single member	Start from 01.01.2003.	Barents Sea, Kara Sea

1.2 The operational TOPAZ system

The TOPAZ model system is an operational real time ocean monitoring and forecasting system covering the Atlantic and Arctic Oceans with 18 to 35 km resolution (EU FP5 TOPAZ project, see topaz.nersc.no, Bertino et al., 2004). The TOPAZ system is built on components of the NERSC model suite. The model system consist of an ocean circulation model, the HYCOM model (Bleck, 2002), and an *ice model* based on the Elastic Visco Plastic (EVP) rheology by Hunke and Dukowicz (1997) for the dynamic part. Thermodynamics is computed using a simple parameterization with a single ice thickness class *(Drange & Simonsen, 1996)*. The ocean model is forced atmospheric data, both now-cast and 10-day forecast with resolution 0.5x0.5 deg, available from the European Center for Medium range Weather Forecasting (ECMWF). Advanced data assimilation techniques are used to incorporate near real-time observations into the coupled ocean sea-ice model. The near real-time observations assimilated in TOPAZ are Sea level anomalies (SLA) combined from 4 satellite altimeters (GFO, ENVISAT, TOPEX-Poséidon, and Jason-2), sea

surface temperatures (SST) from AVHRR, sea-ice concentrations from SSM/I and soon *in-situ* T/S profiles from XBT and Argo floats. The data assimilation method used in TOPAZ is the Ensemble Kalman Filter (EnKF, Evensen 1994, 2003). The assimilation of ocean surface parameters controls the ocean surface dynamics (Brusdal *et al*. 2003) and the assimilation of sea-ice concentrations into the coupled model controls the location of the ice edge (Lisæter *et al*. 2003). This enables the model to represent the general circulation, such as the Atlantic inflow to the Arctic. Results from the model system (Fig. 1) are provided on several formats, including NetCDF files and and OpenDAP. Model results can be visualized online with a Live Access Server (http://topaz.nersc.no/las/servlets/dataset).

a   b
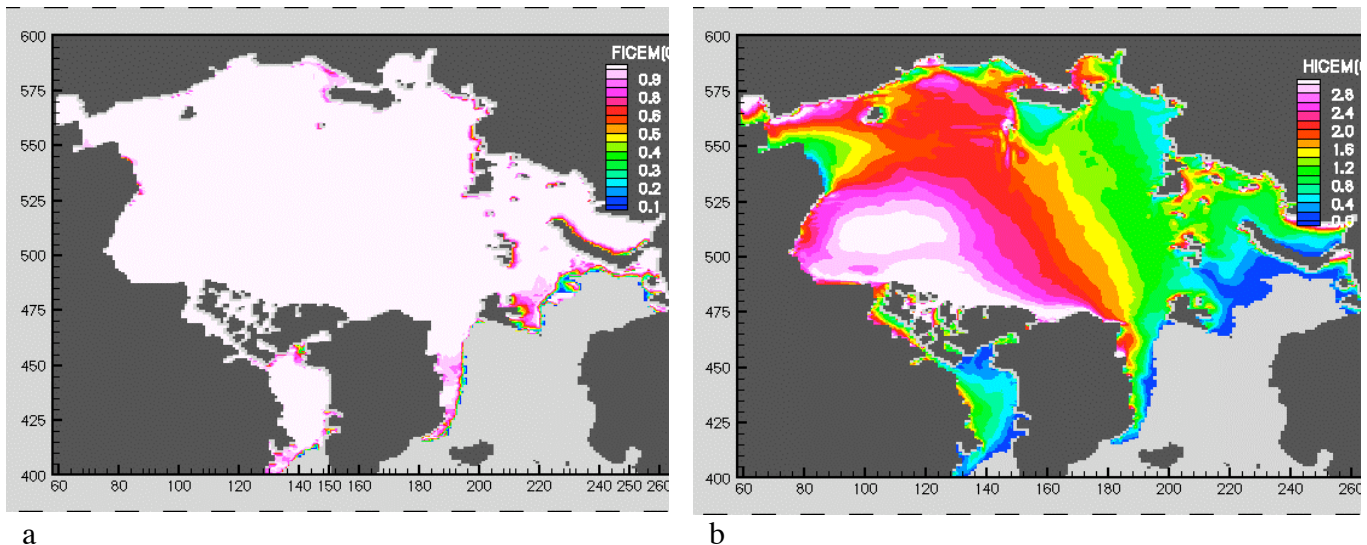
Figure 1. Ice field for 8 April 2003 as derived from the TOPAZ system: a) ice concentration, b) ice thickness

Every week the TOPAZ system produce analyzed maps of current sea ice state, and 10 days sea ice forecasts for the whole Arctic region at a resolution of 20-25 km. Currently, the sea ice forecast products consist of maps of ice concentration, and ice thickness. In Figure 1 we demonstrate results for the 8th of April 2003 from the TOPAZ system. The system has been under refinement and version 2 and is currently running in real-time mode. An example of model results from the upgraded TOPAZ system is provided in Figure 2. These results agree fairly well to the climatology. Since ice concentration is assimilated in TOPAZ, the changes to ice thickness are relatively small. Changes to the ice coverage and location of the ice edge can be seen, however, in the Barents and Chukchi Seas. The assimilation of ice concentration mostly affects the position of the ice edge, which is important to position correctly for operational systems in the Barents Sea, for instance.

The TOPAZ system also computes the ice drift, see Figure 3, The ice drift in the model is partly wind driven and partly driven by the ocean circulation pattern. Two snap shots taken at two different times may therefore differ significantly from each other. Zhang et al. (2003) showed that the assimilation of ice motion observations can have a strong effect on the modeled ice cover, including the ice thickness. Their results showed that the assimilation of ice motion data from SSM/I and buoys improved the ice motion and, through changes in ice motion, the ice thickness fields. In the future sea ice drift will be assimilated in the TOPAZ system as well.
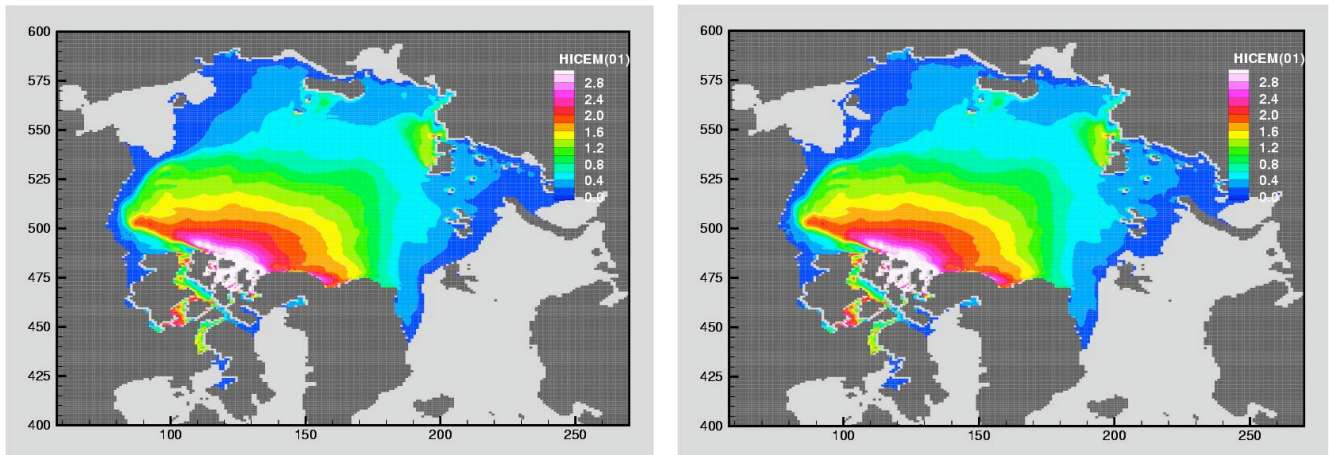
Figure 2. *TOPAZ - 2: Ice thickness fields before (left) and after (right) assimilation on the 26.10 2004*
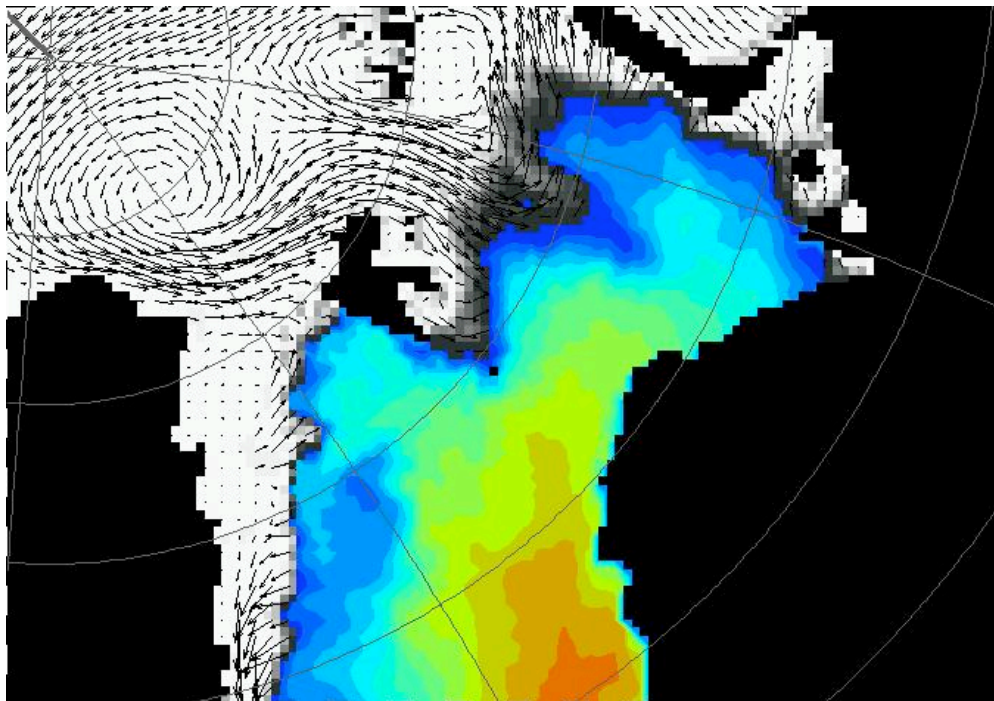
Figure 3. Snap-shot of the sea ice conditions in the Barents Sea and Fram Strait region 26 of March 2004. Ice drift vectors are calculated and overlaid the ice concentration. Please notice that a snap-shot at another time would give significantly different ice-drift situation due to strong dependency on the wind field. Product delivered 18 March 2004.

1.3 North-Atlantic ice-ocean model

As ice information in ice-ocean models has a resolution of at least a couple of km, ice thickness distribution and ridge formation statistics within each grid cell will be important information for safe navigation and operations in these regions. In the North-Atlantic model (50 km resolution) a Multi-Category ice model has been coupled to the HYCOM ocean circulation model. Like the TOPAZ system, the North-Atlantic ice-ocean model is based on the HYCOM ocean model and the

dynamic part of the ice model is based on the Elastic Viscous Plastic (EVP) rheology by Hunke and Dukowicz (1997). For for the thermodynamics a more complex ice representation, that discretizes ice into several ice thickness classes within each grid cell (similar to Bitz, 2001) is used. Multi-Category ice models see the ice cover as a collection of ice floes in different thickness categories. This ice model also describes the redistribution of ice thickness through ridging and rafting within the grid cell. This makes it possible to model the ice thickness probability density function for each grid cell. Example of such thickness distribution is shown in Figure 4a, which shows the total ice concentration in the location of Shtockman, along with the fraction of ice in the intervals 0-0.5m, 0.5-1.0m and so on. The seasonal cycle of total ice concentration is shown, and the figure illustrates how, during the course of a season, the fraction of thick ice increases from October to July (green yellow and red lines). A lot of this thicker ice is due to ice import from the central Arctic Ocean.
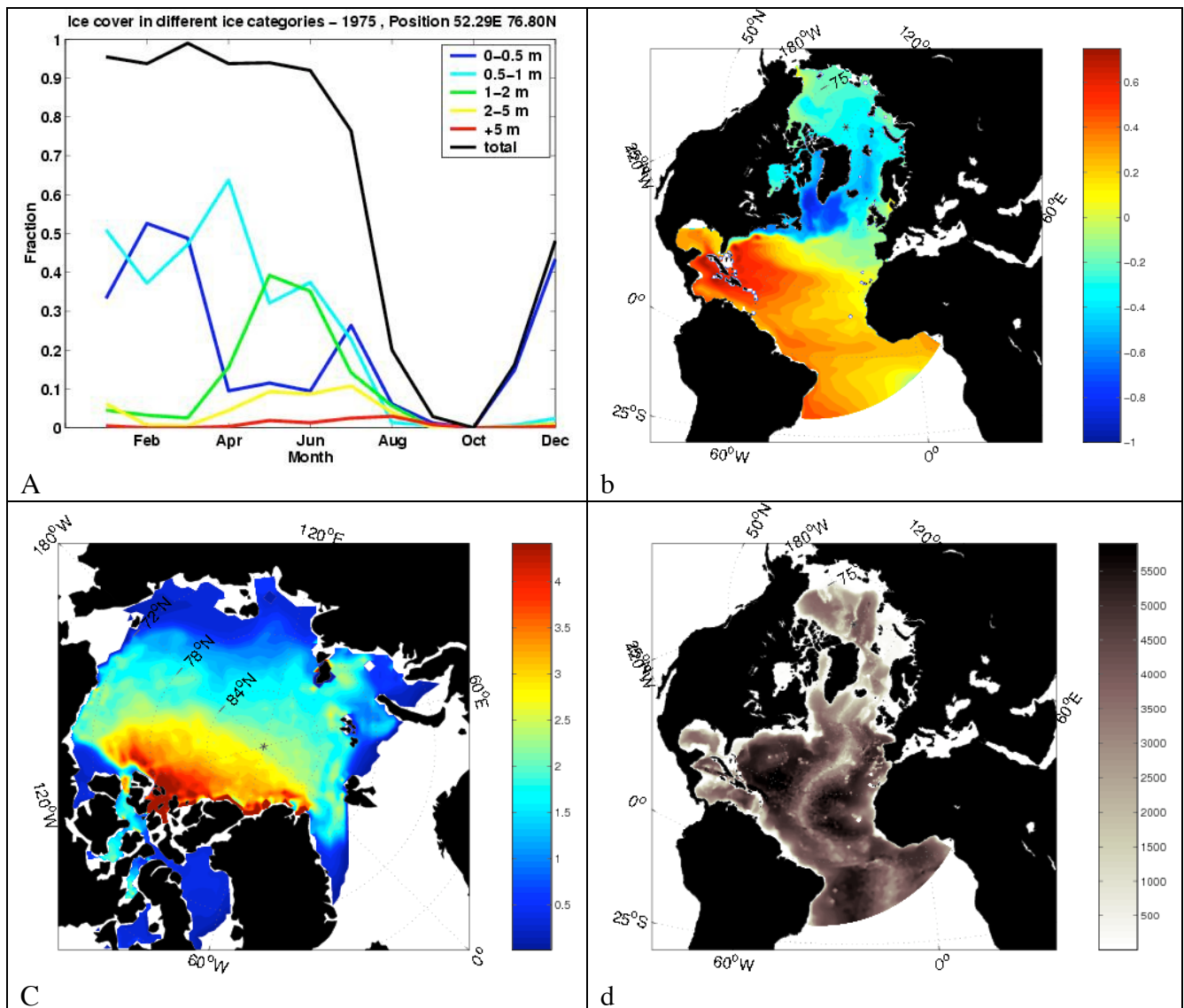

Figure 4. *a: example of ice thickness distribution in a specific location in North-eastern Barents Sea, generated by the Multi-Category ice model at NERSC, b: example of monthly averaged SSH, c: ice thickness year 1990 day 304, d: bathymetry in meter.*

Examples of model output are shown in Fig. 4 b (SSH) and c (ice thickness). This coupled ice-ocean model use atmospheric forcing data from ERA with resolution 1.25x1.25 deg from 1957. The model run in hind cast mode from 1 September 1958 up to 2002. There is no tidal forcing included.

1.4 Global ice-ocean model

The applied model system consists of a global version of MICOM are fully coupled to a dynamic and thermodynamic sea ice module. The dynamical part of the sea ice model uses viscous-plastic rheology (Hibler III, 1979) in the implementation of Harder (1996). The model is configured with a local horizontal orthogonal grid system with one pole over North America and the other pole over central Europe. The horizontal grid resolution in the North Atlantic/Nordic Seas region is about 40 km. There are 26 vertical layers, of which the uppermost mixed layer has a temporal and spatial varying density. The specified potential densities of the subsurface layers are chosen to ensure a proper representation of the major water masses in the North Atlantic/Nordic Seas region.

For the present run the model is initialized with climatologically temperature and salinity fields, a two-meter thick sea ice cover based on climatology, and an ocean at rest. The model is forced with daily NCEP/NCAR reanalysis forcing fields from 1948 with a resolution of 2.5x2.5 degree. Model runs from 1948, and is operated in a synoptic hind-cast simulation mode. Examples of model ice output are provided in Figure 5. These plots are modeling the ocean-ice state in March 1999. Furthermore histogram of regimes of ice thicknesses has been calculated.

The output from the ice module will be validated with available data. This model system is integrated forward in time when forcing fields are available. Besides validation activities, the model results will be used to characterize the temporal and spatial changes in the ice thickness. This can provide important information where to put future in-situ sensors.
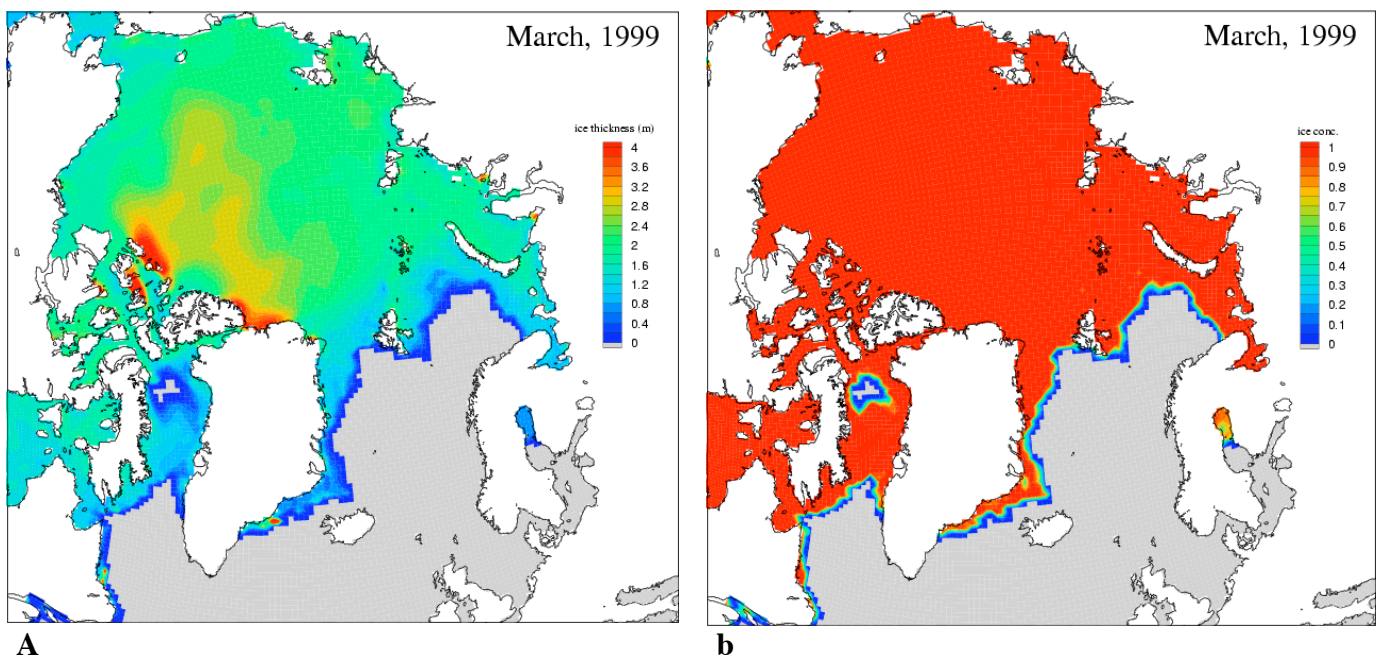

Figure 5: a: sea ice thickness (m), and b: ice concentration produced by the global model for March 1999.

2. The HYCOM model formulation

Ocean general circulation models have traditionally been categorized based on their vertical representation. This involves, amongst others, the discretization in z-level coordinates, the terrain-following -coordinates, and isopycnal models using density as the vertical coordinate. These models have advantages and disadvantages depending on their applications, and there is now a consensus that a "hybrid" model combining the best parts from all of these will be the model for the future.

Ideally, an ocean model should retain its water mass characteristics for centuries of integration (a characteristic of isopycnic coordinates), have high vertical resolution in the surface mixed layer for proper representation of thermodynamical and biochemical processes (a characteristic of z-level coordinates), maintain sufficient vertical resolution in unstratified or weakly-stratified regions of the ocean, and have high vertical resolution in coastal regions (a characteristic of terrain-following coordinates).

The hybrid coordinate is isopycnal in the open, stratified ocean, but smoothly reverts to a terrain-following coordinate in shallow coastal regions, and to a z-level coordinate in the mixed layer and/or unstratified seas. The hybrid coordinate extends the geographic range of applicability of traditional isopycnic coordinate circulation models toward shallow coastal seas and unstratified parts of the world ocean. In doing so, the model combines the advantages of the different types of coordinates to optimally simulate both coastal and open-ocean circulation features.

Such a model, i.e, the Hybrid Coordinate Ocean Model (HYCOM) has recently been developed by Bleck (2002), based on the previous Miami Isopycnal Coordiante Ocean Model (MICOM) by Bleck et al. (1992). This latest HYCOM model is adopted in this study with the exception of the global model which uses MICOM.

2.1 Vertical coordinate scheme

The vertical movement of water masses can be divided into a Lagrangian movement where a coordinate surface is moving with the water in the vertical, as in an isopycnal model, and the movement of water through the coordinate surface as is done in all models with a fixed vertical coordinate system, e.g. z-level models and -coordinate models. HYCOM includes both representations of vertical movement of water masses and allows for a combined use of material coordinate surfaces and fixed coordinate surfaces. An example of a vertical section of temperature from HYCOM is shown in Fig. 6.

The algorithm exploits the fact that all layers have an assigned reference density (as in isopycnal models). Further, one defines a minimum layer thickness for all layers except for the deep layers intersecting the bathymetry. Whenever the upper isopycnal layer approaches this minimum thickness, because water with this reference density ceases to exist in a vertical column, this layer is used as a vertical level coordinate providing resolution in the mixed layer. Further, this level coordinate is located at a depth according to a predefined rule. The algorithm results in a stack of levels located from the surface and downwards with a specified resolution. As a consequence, the model allows for arbitrary high vertical resolution near the surface by adding a sufficient number of light (and therefore always mass-less) layers to the model.

Thus to summarize, based on the number of layers defined and their chosen reference densities, the layers will distribute themselves in the vertical, starting with isopycnal layers from the sea floor and upwards towards the surface. The layers with reference densities lighter than the existing water

masses in the present water-column will be stacked from the surface and downwards with a specified vertical resolution, and used as z-level or sigma-level coordinates.
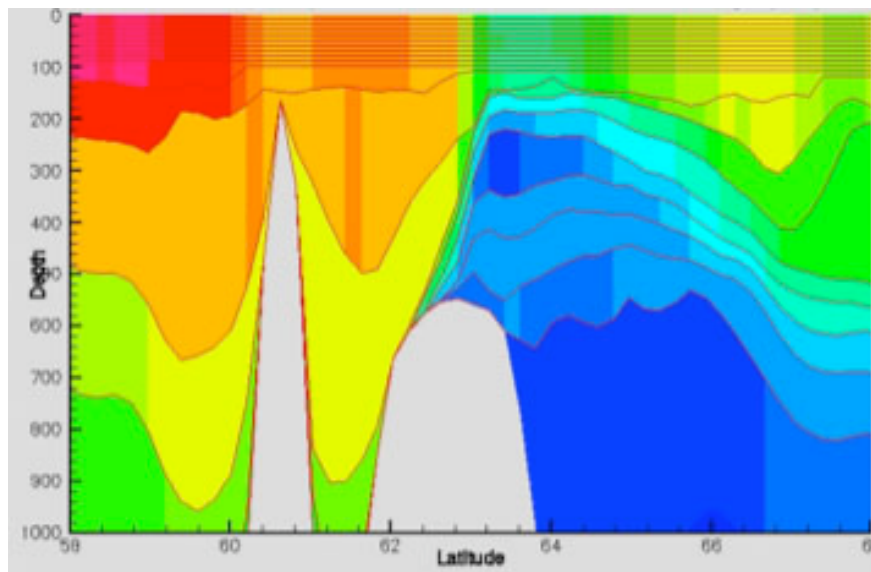

Figure 6*: Typical "hybrid" temperature section of Hycom model across Faero-Iceland Ridge (Nov). Note the high vertical resolution at the interface between cold (blue) and warm (yellow) water.*

2.2 Mixing processes in HYCOM

Vertical mixing in HYCOM is a combination of cabbeling and restoration processes and the explicitly prescribed physical mixing.

The horizontal advection and mixing of layer thicknesses, tracers and momentum is computed using two dimensional algorithms operating on individual layers (as is also done in MICOM). However, the advection of layer thicknesses in the continuity equation will introduce a vertical movement of the layer interfaces, also among the level coordinates near the surface. Further, horizontal diffusion of temperature and salinity in an isopycnic layer may lead to a deviation from the reference density. The nonlinearity of the equation of state implies that the mixing of two water masses with different temperature and salinity properties but the same density, may result in a new water mass with a different density.

The prescribed vertical mixing is solved using the KPP vertical turbulence closure scheme developed by Large et al. (1994). The scheme computes the vertical mixing coefficient over a vertical column in the model, and takes into account the effect of wind-induced mixed layer turbulence and additional mixing parameterization for processes such as internal wave breaking, Richardson dependent vertical current shear, salt fingering and double diffusion. A background vertical mixing coefficient ensures the presence of a low diapycnal diffusion in the deep ocean. The scheme uses an algorithm to compute the vertical diffusivity in a water column, and thereafter a one-dimensional diffusion equation is solved for temperature, salinity and momentum.

At every time step, an algorithm restores the correct location of the coordinate surfaces. Among the isopycnal layers in the deep ocean there is a restoration towards reference densities, an effect called

cabbeling, where a small amount of water is mixed between adjacent layers to restore the reference densities. For the level coordinates near the surface, water is moved/mixed between layers to restore the layer interfaces to their predefined locations in depth. This process is designed to conserve temperature, salinity and momentum in a water column.

3. The high-resolution Barents Sea model

3.1 Background

A resolution of about 20 km, which is used in TOPAZ, is too coarse to resolve mesoscale processes of importance for the local representation of ice edge configuration, ice drift and ice concentration, and correspondingly important for the ice thickness distribution. Local and detailed sea ice information, including ice thickness, will in future be essential for safe navigation and operations in these regions. To support these needs a regional high-resolution coupled ice-ocean model has been established for the Barents Sea and the Kara Sea with a grid cell of about 5 km. When we have gained experience with 5km resolution, it will be decided if there is a need to increase the resolution. Like the TOPAZ system, the Barents Sea is based on the HYCOM ocean model. The dynamic part of the ice model is based on the Elastic Visco Plastic (EVP) rheology by Hunke and Dukowicz (1997).

In order to obtain an accurate now-cast and forecast in the Barents Sea, the whole North Atlantic and Arctic basins systems need to be included in the model, although with less precision. This is done by nesting, which means that the high-resolution model takes its boundary conditions from the coarser model. The coupled ice-ocean model system is nested in the ocean layers and in the ice layer. Boundary conditions from the large-scale models are imposed on the regional models using a one-way nesting scheme where the boundary conditions of the regional model are relaxed towards the output from a coarser large-scale model. In addition one needs to specify the barotropic (depth-averaged) transport from the outer model into the regional model.

3.2 Nesting procedures and boundary conditions

Open boundary conditions and nesting in ocean circulation models are considered more as an art than real science. The main problem is that for a model with open boundaries the number of boundary conditions is dependent on the structure of the flow field penetrating the boundary. There are actually four cases, which must be considered, i.e., inflow or outflow and for each of these one can have supersonic or subsonic velocities. To avoid dealing with the problem of exactly specifying the boundary conditions in a "proper" nesting scheme, most approaches use some kind of boundary relaxation towards the outer model solution. This results in what one normally would call the one way nesting schemes where the boundary conditions of the regional model are relaxed towards the output from a coarser large scale model. For the slowly varying variables, i.e., baroclinic velocities, temperature, salinity and layer interfaces, this is a fully appropriate way to include the boundary conditions. For the barotropic variables the relaxation approach requires careful tuning to avoid reflection of waves at the open model boundaries. In HYCOM the barotropic model is a hyperbolic wave equation for pressure and vertically integrated velocities. Following an approach outlined by Browning and Kreiss (1982, 1986), it is possible to compute the barotropic boundary conditions exactly while taking into consideration both the waves propagating into the regional model from the external solution and the waves propagating out through the boundary from the regional model. The scheme has been tested extensively and has shown no problematic behavior yet. In addition, it also made it fairly simple to include the tidal forcing on the barotropic mode.

The practical implementation of the nesting scheme is based on communication through files stored on disk. The outer model dumps the solution interpolated to grid points in the relaxation zone of the regional model every 6 hours. For the baroclinic mode, which changes slowly this is considered to be high resolution in time. It should also be sufficient for the barotropic mode as long as the outer model does not contain tides. The regional model reads the files every six hours and uses interpolation in time to specify the relaxation boundary conditions at every time step. The communication between the grids is general and there is no restriction on the relative orientation or resolution of the grids.

The Barents Sea model receives boundary and initial conditions from the TOPAZ model. We also save some spin-up time by restarting the nested model from a coarser resolution model such as TOPAZ. The bathymetry was generated from the GEBCO, 1-minute resolution topography. GEBCO showed improvements in the shallow regions by comparison with the older ETOPO-5 database. The detailed Barents Sea model domain and bathymetry is shown in Figure 7.
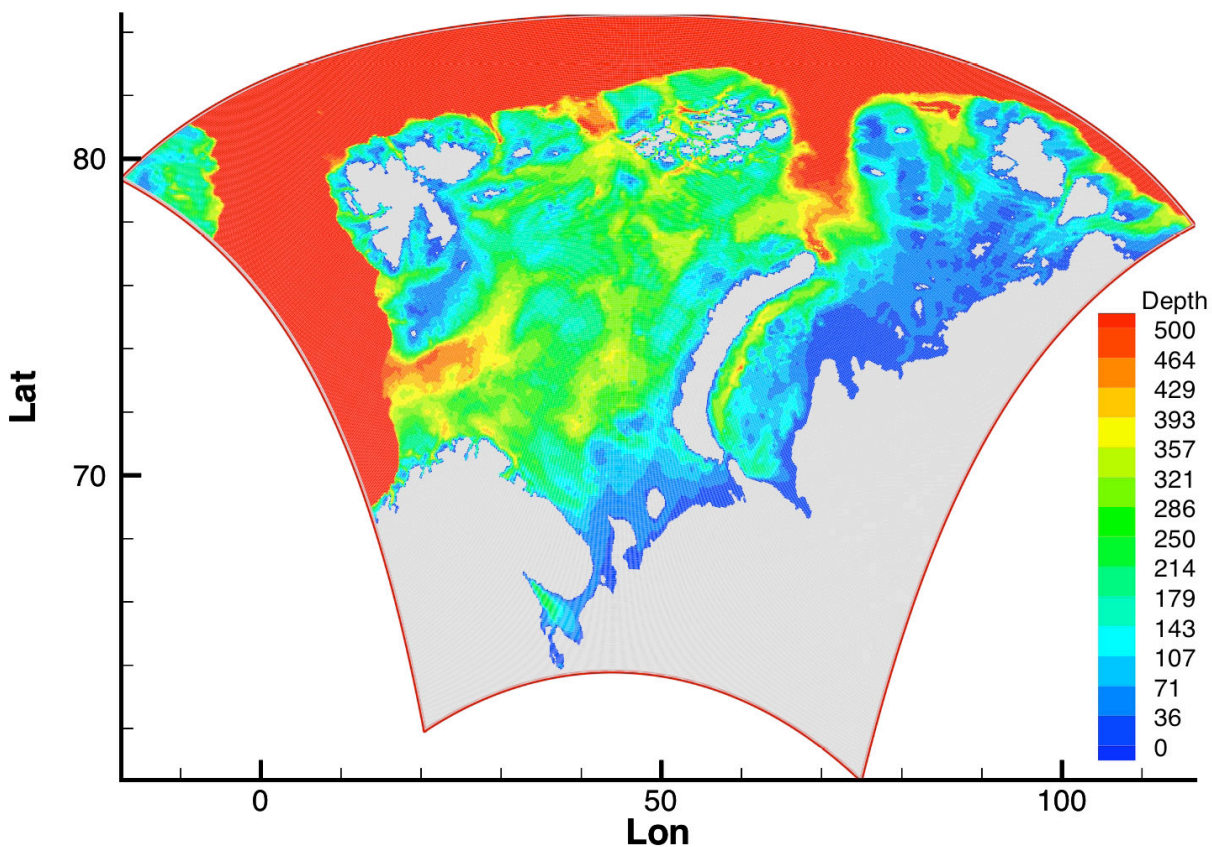

Figure 7: *The domain of the high resolution Barents Sea model. The colour coding indicates the bathymetry.*

We stored the nesting conditions from the TOPAZ model every 6 hours. The nesting conditions include baroclinic velocities, temperature, salinity, layer interfaces and barotropic velocities and pressure. Output from the model is horizontal and vertical fields of the whole area, and some defined grid-points, the station Stockman and in addition to some other chosen points. As the model takes the nearest grid point, this can not be more than around 3 km from the station, as the resolution of the model is 4.5-5.5km. Neither the TOPAZ nor the Barents Sea model use data assimilation in the 1979 period because of the associated costs in manpower and CPU.

Fluxes from the large-scale model

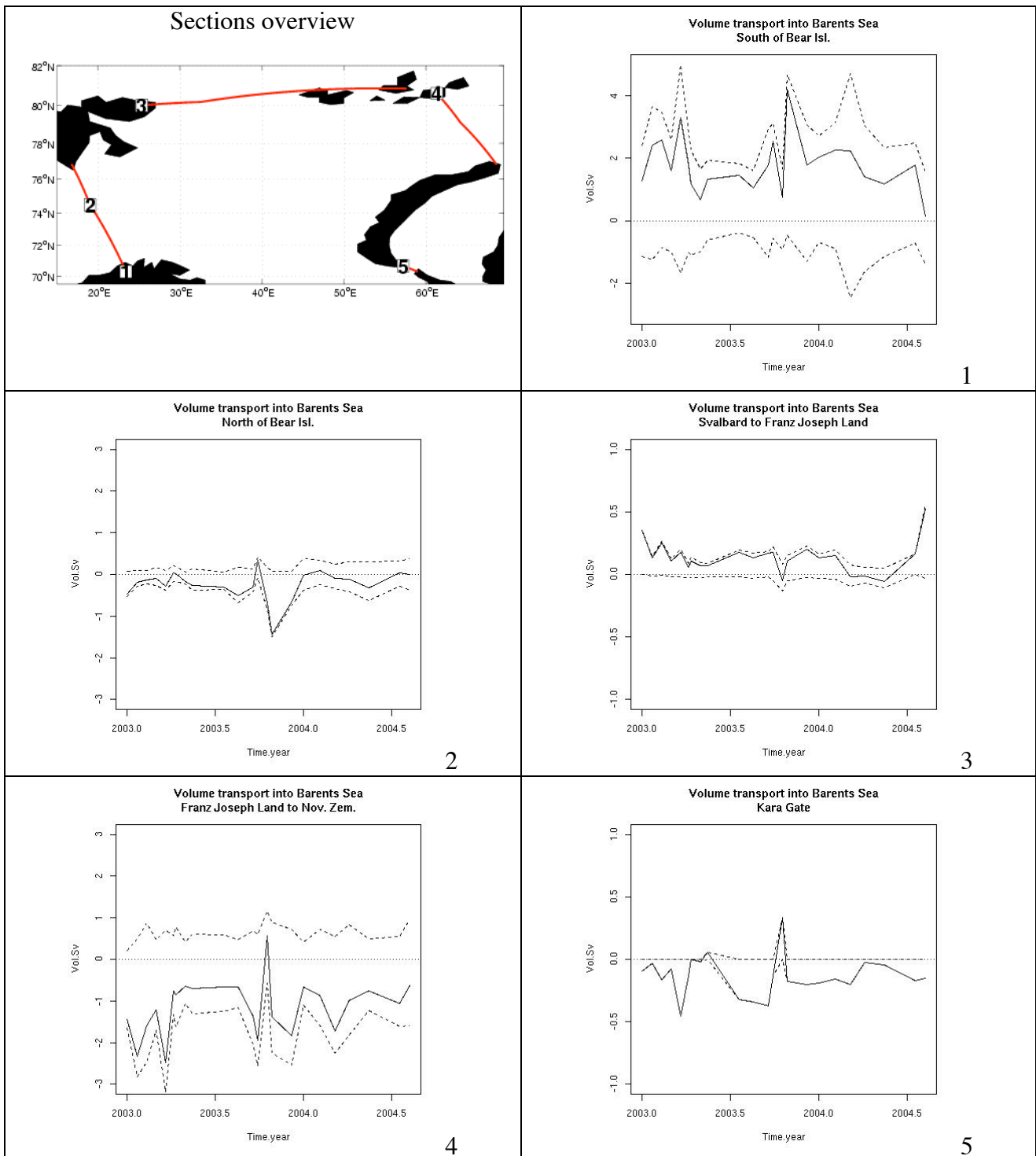***Figure 8****: Fluxes entering and exiting the Barents Sea from the TOPAZ model. Sections 1 to 5 are oriented clockwise (see overview map). Positive fluxes are flowing into the Barents Sea and negative fluxes are flowing out (fluxes are coming in through section 1 and 3, and out through sections 2, 4 and 5). The solid line is the net flux and dashed lines are the positive and negative fluxes.*

The fluxes are computed during a 2-years free run of TOPAZ (2003-2004) and compared to the literature. The results are summarized in Table 2 and indicate that the model behaves qualitatively well. Given the large interannual variations in the region, a longer model run should be performed to cover the whole period when the measurements were taken. This has not been done in the present work but will be performed within the Mohn-Sverdrup Center's activities.

Table 2: Summary of TOPAZ fluxes in the Barents Sea against observations

Section	Reference	Model	Observed
1: Melkøya – Bear Island	Ingvaldsen *et al.* (2004) and Blindheim (1989)	1 Sv (summer) 3 Sv (winter)	< 1.8 Sv (summer) < 2.2 Sv (winter)
2: Bear Island – Spitzberg	Ingvaldsen *et al.* (2004)	0.5 Sv	1 Sv
3: Spitzberg – Franz Joseph Land	Loeng *et al.* (1997)	In: 0.2 Sv Out: 0.1 Sv	In: 0.4 Sv Out: 0.1 Sv
4: Franz Joseph Land – Novaja Zemlja	Schauer *et al.* (2002)	In: 0.6 Sv Out: 0.5 – 3 Sv	In: < 0.3 Sv Out: 0.6 – 2.6 Sv
5: Kara Gate	Loeng *et al.* (1997)	In: 0 to 0.3 Sv Out: 0 to 0.5 Sv	In: 0.1 Sv Out: 0.05 to 0.7 Sv

Tidal boundary conditions

The tides have been specified as a barotropic forcing on the open boundaries for the regional model. This was fairly easy using the nesting boundary conditions explained in the previous section. The data set used has been released by the University of Texas and is based on assimilation of several years of altimeter data collected by the TOPEX satellite.

River outflow

The rivers outflows are based on monthly climatologies. Rivers are placed on the closest point on the domain to where the riverfluxes are measured. The regional model has eleven rivers where the four bigger are: Northern Dvina, Pechora, Ob and Yenisey.

Sea Ice

A dynamic and thermodynamic sea ice module is coupled to the ocean model. The ice dynamics are based upon elastic-viscous-plastic (EVP) rheology developed by Hunke and Dukowicz (1999). Thermodynamics are computed using a simple parameterization with a single ice thickness class (Drange and Simonsen 1996).

3.3 Hydrographic validation data

Collection

Ocean data in the Barents Sea have bee collected in the period 1900-2000 by Arctic and Antarctic Research Institute (AARI) within the INTAS project entitled "The Nordic Seas in the global climate system". The resulting database is a unique gathering of stations from western sources and former Soviet sources. The repartition over time of the 2.5 million stations and their different sources is shown in Figure 9.

Initial oceanographic datasets (DS) were requested from different data centers, institutions and international projects sources. At the moment total amount of initial DS come to 25 with about totally 2.5 millions of oceanographic stations. Some of the data sources /sets were replaced by more recently published data. For instance Climatic Atlas of the Arctic Seas 2004 (CLA2004) was used instead 'ClimBar' and 'BarKode'. CLA2004 themselves pass the merging procedure for data from original CD and data prepared by A. Zuev (Murmansk Marine Biological Institute MMBI) with control and elimination of duplicates. Several similar initial DS were merged together to reduce the number of duplicate data used. All original DS were loaded into separate databases under the Interbase server. Structure of metadata and database tables was designed for data storage in oceanographic database. Although it was planned to process only temperature, salinity and oxygen profiles all other chemistry parameters have been stored, but without subsequent quality control. Program application (ODB3ALoad) was created for data conversion from original to Interbase format, initial quality control and different kind of processing procedures. International codes were used for country and vessel identification. Because different initial DS contain similar but not the same codes a new joint codes table was generated on the base of all initial sources.
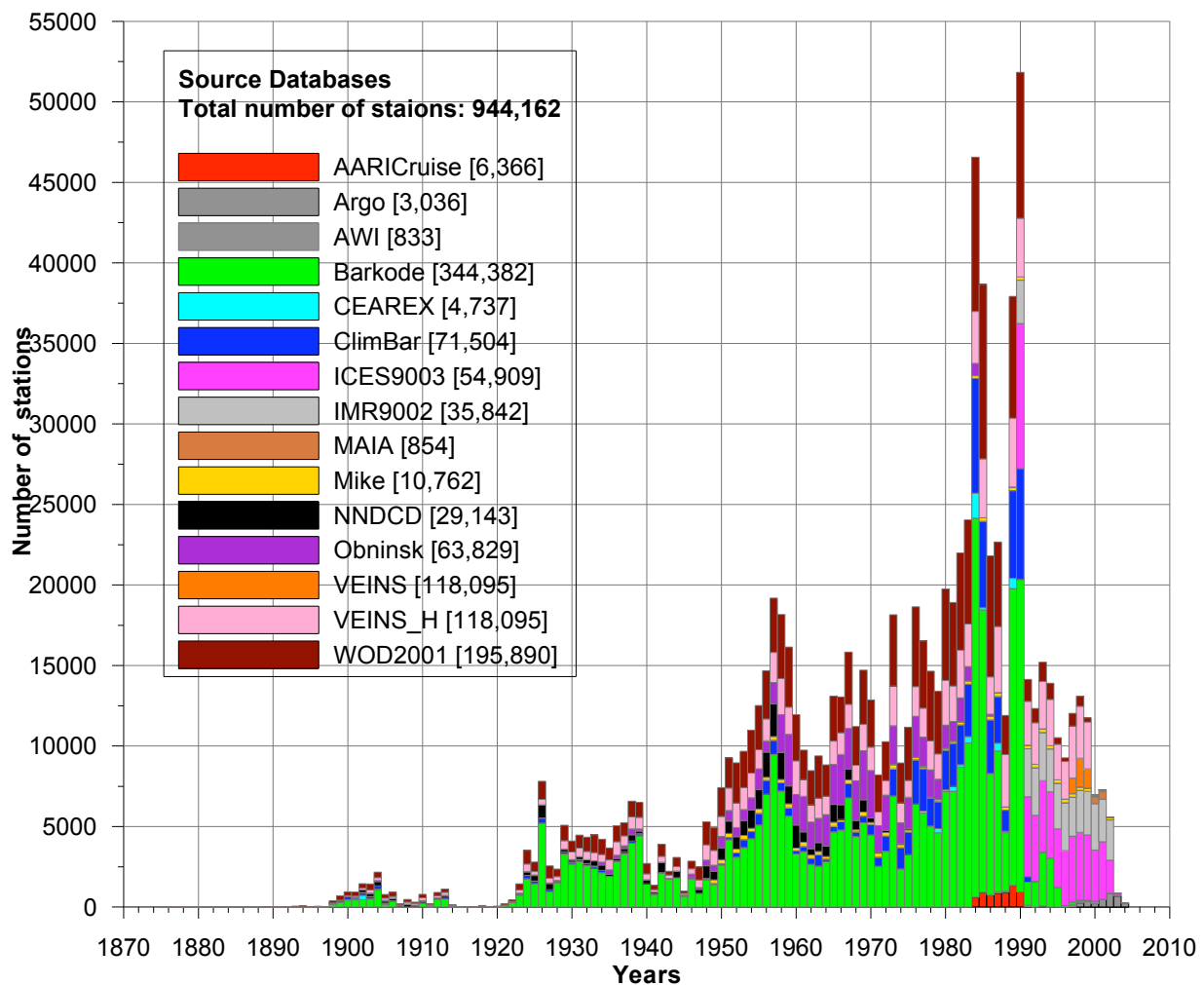

Figure 9: *Temporal coverage of the hydrographic database. Note the shutoff of Russian data after 1990 (Ref. INTAS project "The Nordic Seas in the global climate system").*

The existing Barents Sea database (Climatic Atlas of the Barents Sea 1998: Temperature, Salinity, Oxygen. NOAA, 1998; Biological Atlas of Arctic Seas 2000. Plankton of the Barents and Kara Seas. WODC, 2000) was extended by the new oceanographic observations carried out in the recent expeditions of MMBI and cooperating organizations and also by the archive data dating from the first half of 19th century. Exchange of oceanographic data and methods has been undertaken between AARI and MMBI.

Processing

The hydrographic data have been quality checked, duplicates have been removed and then the data gathered by month have been interpolated on a regular Lat-Lon-depths grid by ordinary Kriging (A. Pnyushkov, AARI/NERSC, personal communication). A climatology for the region has been produced as well as estimated maps provided on request for the project period in 1979. This task has also been performed at AARI under the "Nordic Seas" INTAS project.

Initial quality control was applied for all databases with region reduction to the Nordic Seas area. To exclude data biases a limitation was set to use only the profiles with three or more measured levels for temperature or salinity. Next limitation was that data with low accuracy (MBT, XBT) were eliminated for station where instrument type was determined. The limitations lead to decreasing of the number of stations, especially surface managements. It is planed to compose separate database containing only upper layer measurements. Initial quality control consists on parameters range control, levels control (minimum number, sequence, duplicates, maximum number), stability checks and duplicate control inside database. Depending on algorithm quality control flags were set on station or on measured parameter value. After all procedures the total number of stations inside all initial databases for the Nordic Seas area comes to almost one million.

Special program module was developed to merge the initial databases with duplicates control. The purpose was to find best metadata and profiles composition for each station from all available variants. All stations with the same date lays within ± 1' coordinates around the stations were checked for duplicates. Hierarchy of algorithms was developed for automatic duplicates identifications including absolute (all metadata and profile coincide), full (metadata partly and all profile coincide), TSO2 (metadata partly and temperature, salinity and oxygen profiles coincide), interpolated variants (profiles cross interpolation by pairs), reduced resolution CTD (checking of nesting), multi-day stations. Criterion for interpolated and different resolution profile was set 0.01°C, 0.01psu and 0.01 ml/l for temperature, salinity and oxygen respectively. Important concept is that automatic duplicate control produce improved merged station presentation (both metadata and profiles) in coincidence with a priory initial databases hierarchy. If all automatic algorithms were failed to find duplicates – expert control was applied. The advantage of the program module is that more then 90% of duplicates can be detected automatically. Actually all data was divided on 12 pieces for each month and processes by AARI team members using described software. This work is not finished yet. Later on all new data will be added into the merged database with similar duplicated control.

Interpolation at the standard levels and standard deviation control modules also embedded into ODB3ALoad application. Linear, Lagrange and Reiniger-Ross methods are applied depending on measured levels vertical distribution and depth difference between levels. Flagged low-quality measurements are illuminated prior interpolation. Standard deviation control allows to set flags on data with value outside 3, 4 or 5 standard deviations. The algorithm starts from sample definition around selected station. Initial criterions for selection are 50km in space around the station and ± 10 years in time. On each step the normality of parameter distribution is estimated for sample (Hi-criterion and Cholmogorov-Smirnov criterion for small sample less then 35). If the normality

condition is not complied at first step the sample size enlarged by 50km in dimension and 10 years in time, but not more that 300 km. If normal distribution not found – value not analyzed for standard deviations. To avoid annual variations algorithm applied for monthly data.

The next program application under developing is a visual user interface for data access in oceanographic database (ODB3A). It represents different tools for data selection, processing and visualization. At the moment application allows make different kind of selections by metadata fields (coordinates, date, time, country, vessel, depth and so on), advanced selection criterion (within distance around defined point, defined irregular-shaped area, along section, interactive selection on map), get different kind of data temporal and spatial statistics in tabular and graphical form (yearly, monthly, by parameter, country, vessel, source and so on), unload selected stations in text format.

An essential module included into application to produce parameters, anomalies and average fields is an objective analysis based on the methods of simple and ordinary kriging. This module includes the point and block variants of kriging system with anisotropic model of theoretical variogram and technology of direct access to database. At the moment four function types (liner, spherical, exponential and Gaussian) are being used as theoretical fits of empirical variogram. A method of spatial structural function decomposition is realized also that allows us to determine large and short scale variations into the fields under study. Using of optimal interpolation routine allows us estimating of interpolation error that is necessary for anomalies and mean maps computing.

3.4 Discussion of model simulation results

This chapter presents the results from a four months integration of a high-resolution model for the Barents Sea Region, in order to evaluate the potential of using this model in developing an iceberg drift model. The first half of the year 1979, the Barents Sea ice condition underwent extreme sea ice conditions. The ice edge at some locations was far west compared to the extreme year of 1966. This was due to high air pressure prevailing a strong outflow of cold air from the continent (Vinje,1979).

Hydrographic model-data comparison

In Figures 10 and 11, we show simulated model temperature and salinity and comparison with observed data for February 1979 at depths of 5, 10, 20 and 100m. The observational data has been kindly provided by A. Korablev from the Arctic and Antartic Research Institute in St Petersburg. We see clearly that the Polar Front, identified by the transition zone between relatively warm and saline water and relatively cold and fresh water, is well simulated by the model compared to observations. The gradual decrease of temperature from the western to the eastern part of the Barents Sea is also well defined in the model. In the south-western part of the Barents Sea the model is much colder than the data, which might indicate a weak North Atlantic inflow in TOPAZ. The salinity plots shows the clear signature of the Norwegian coastal current along the coast of Norway and the North Cape Current in the vicinity of 72 degrees north. The front of the North Cape current is not systematically well located and the differences between the data and the model are about 0.2 psu. In the surface layer, along the coast of Murmansk, a clear salinity anomaly is not captured by the model. This can be explained by the fact that the model uses monthly average climatology for the rivers runoff, which might be too imprecise. The extreme northward extension of ice-free bight north and northwest of Svalbard is maintained by a relatively strong West Spitsberg current transporting warm Atlantic water to the north. The model catches this feature as shown in Figures 12 a and b).
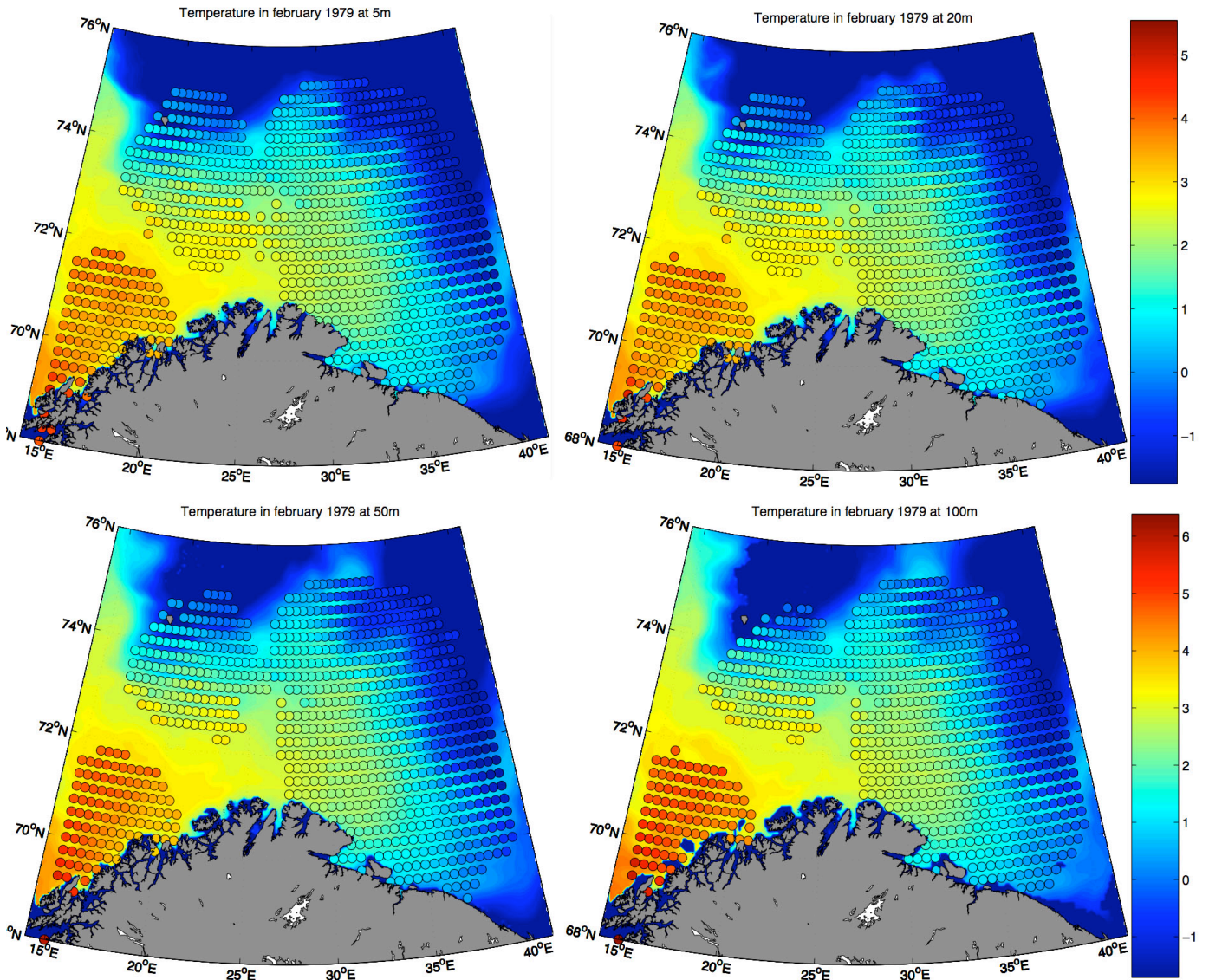
Figure 10*: Ocean temperature mean fields for February 1979: Model results (raster image) and observation results (circles) at 5, 20, 50 and 100m depth.*
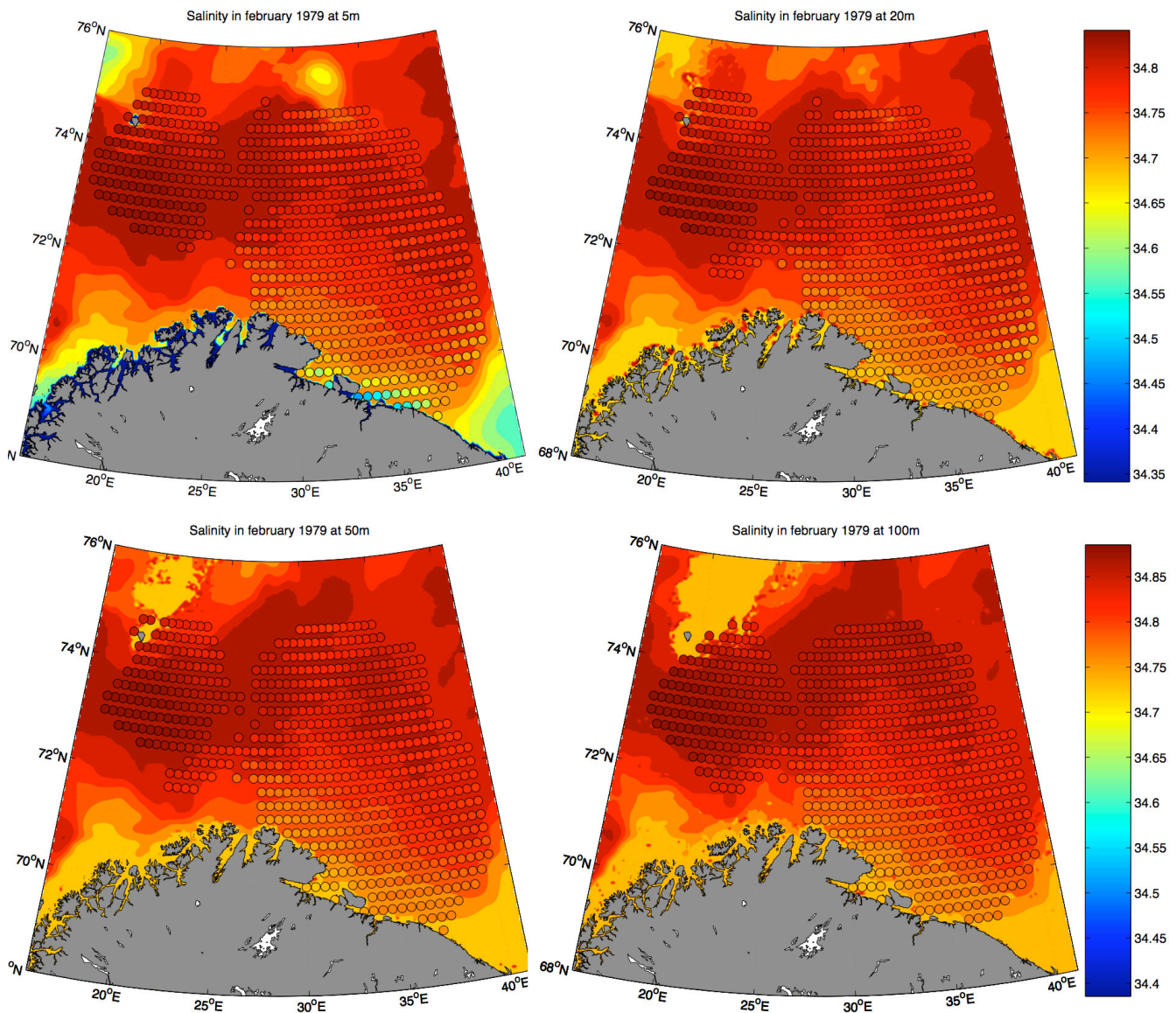
Figure 11: *Ocean salinity mean fields for February 1979: Model results (raster image) and observation results (circles) at 5, 20, 50 and 100m depth*

Sea-ice

The sea ice concentration has been compared with the Special Scanning Microwave Imager (SSM/I) satellite passive microwave ice concentration with a resolution of about 25 km. The algorithm used to estimate total and multiyear ice concentration from passive microwave and surface air temperature measurements has been developed by Svendsen et al. (1983). The results for each month are shown in Figures 12a, b, c and d. Those results shows clearly that the "shape" of the ice edge is respected in the model but for the first 3 months the model predict its location less sea ice than the SSMI data. In April, this not the case so we cannot conclude on a systematic tendency of the model. Thus, this difference in the ice edge location is in the order of few tens of kilometers. Such a performance is satisfactory for a free-running model of about 5 km resolution and is possibly the best presently available.
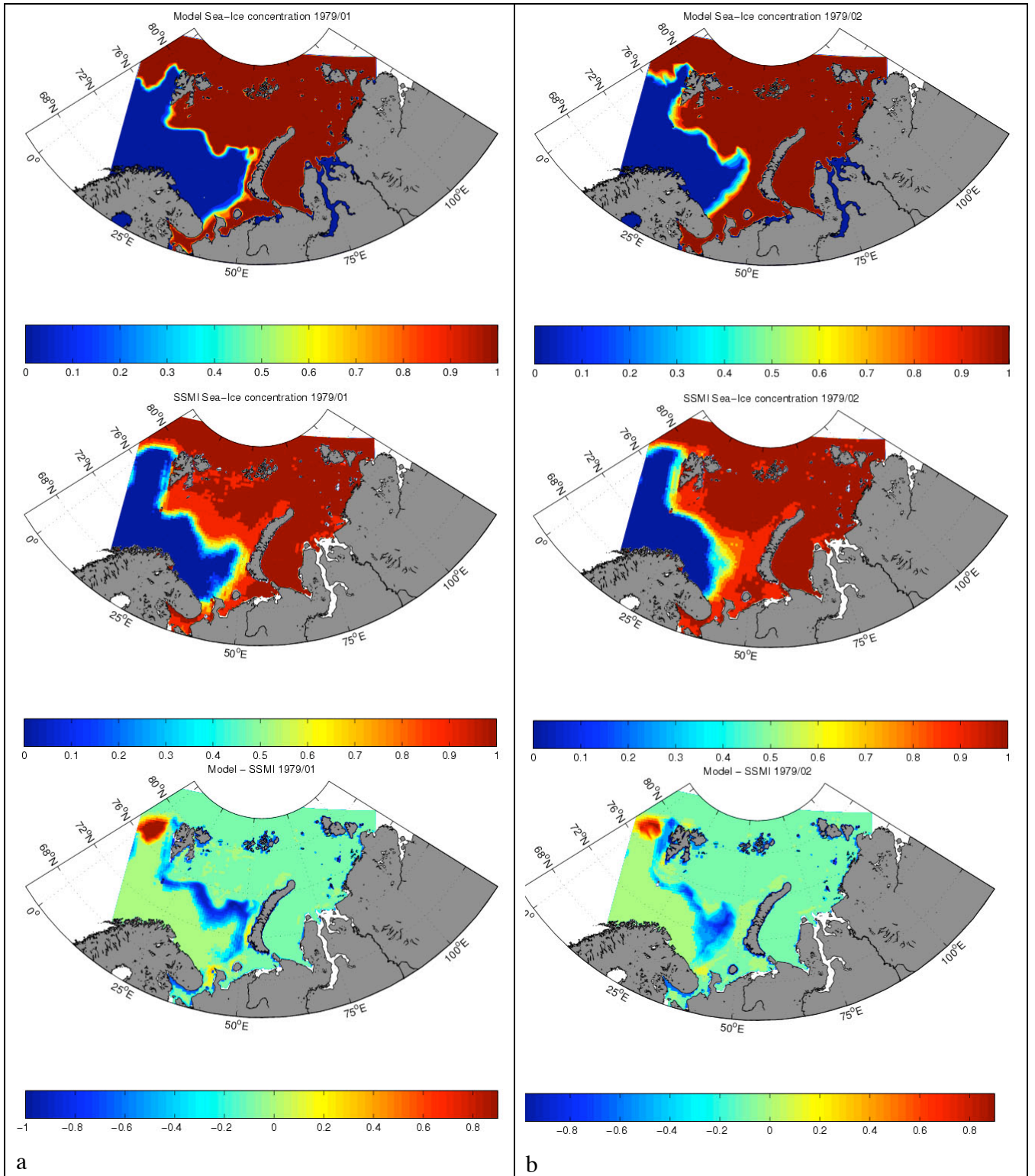
Figure 12 a and b*: Mean Sea ice concentration in January (a) and February (b) 1979: Model simulations at the top, observations in the middle and the difference between the two at the bottom. Positive difference means that the model gives higher ice concentration than the observations.*
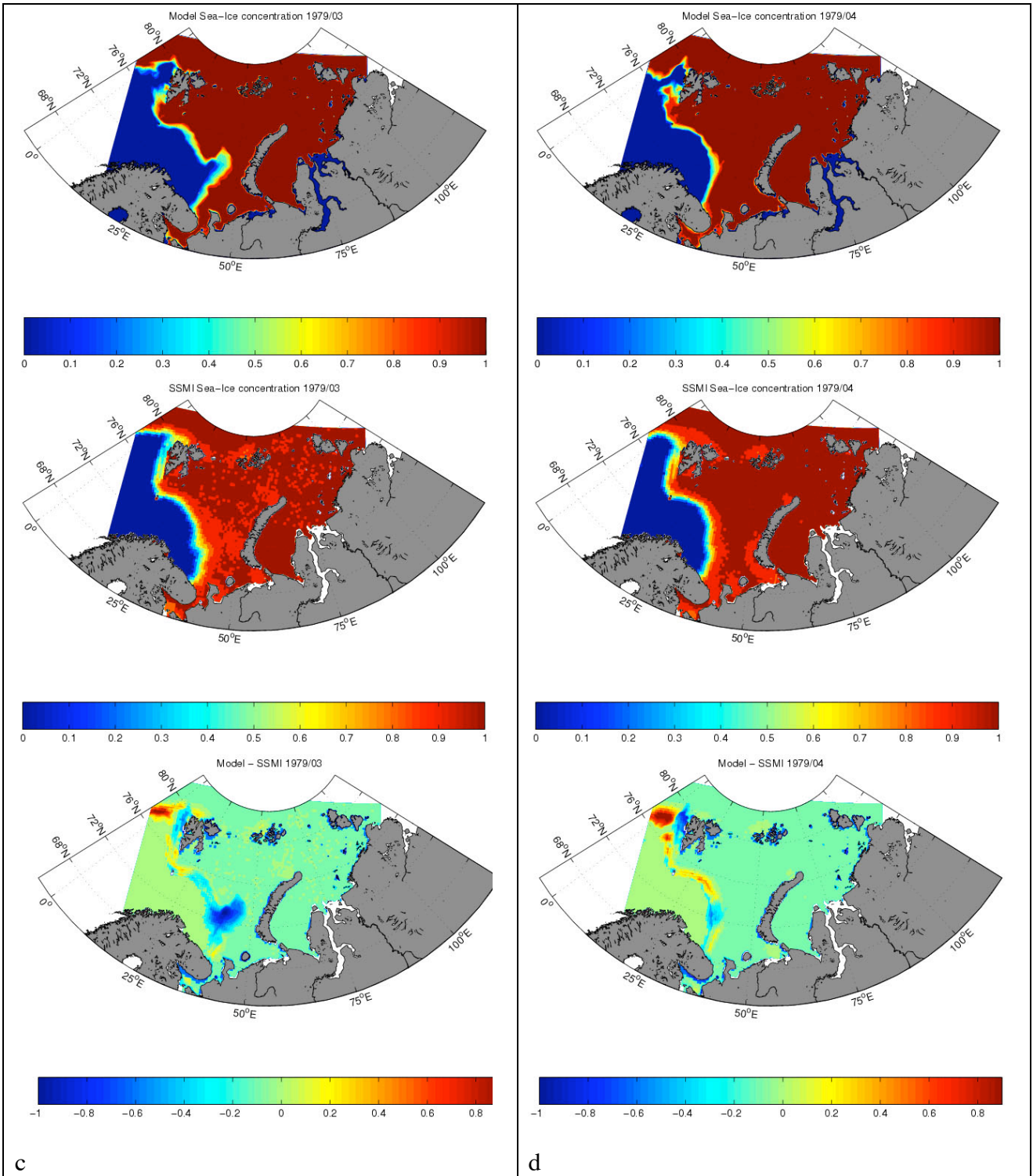
Figure 12 c and d: *Mean Sea ice concentration in March (c) and April (d) 1979: Model simulations at the top, observations in the middle and the difference between the two at the bottom. Positive difference means that the model gives higher concentration than the observations.*

As a rule of thumb, sea ice drifts with a speed from 2 to 8% of the wind speed and at an angle of 15 to 25% to the right of the wind direction depending on the ice surface roughness and the direction and magnitude of the ocean currents. Deviation from those values occurs where ice is influenced by the presence of coastlines or islands and when sea ice is compacted and has no place to move. Figure 13 illustrates the characteristics of the sea ice velocities in Stockman grid cell for the first 25 days of April 1979. We see clearly that at high wind stress, the sea ice tends to follow the wind, which is not the case when the wind is weak. It is then influenced by other processes, mainly the tidal currents.
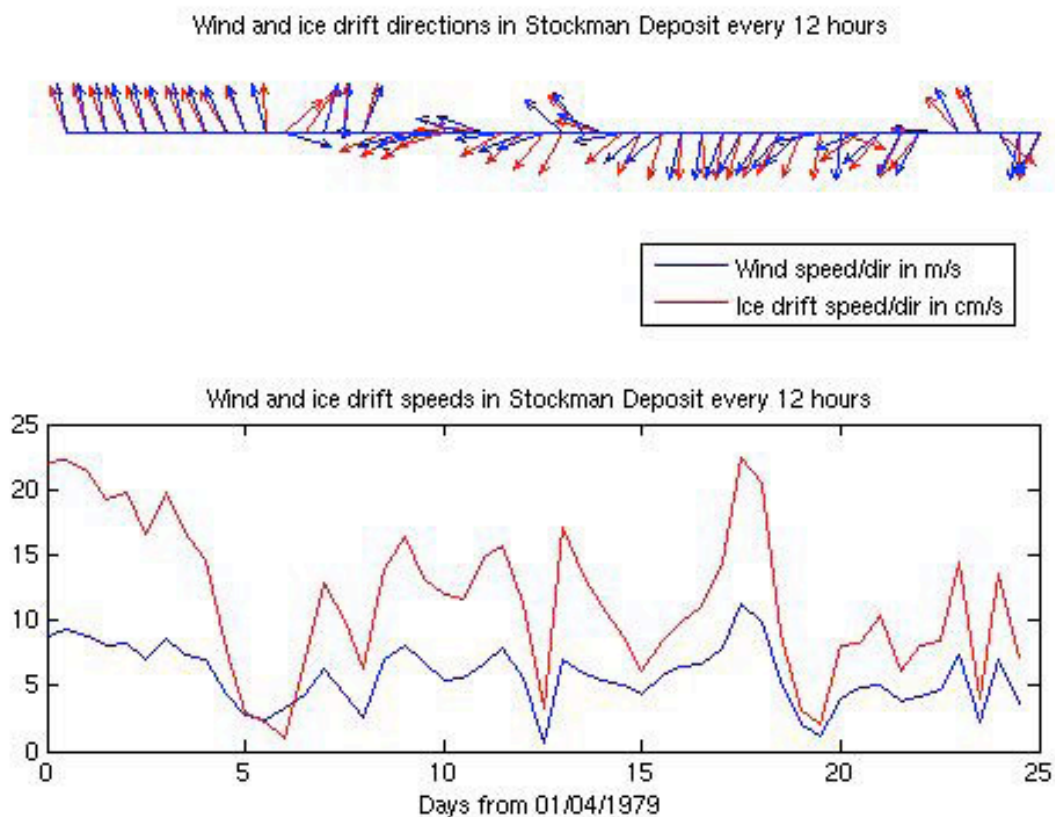

Figure 13: Comparison between wind stress and ice drift in Stockman field for April 1979.

Preliminary conclusion

The first results shows that the model catches the realistic features of the water mass fluxes, hydrographic fields the sea ice conditions in the Barents Sea as compared to observations. Further work must be done to check how well the model simulates other properties such as the mesoscale activities and the accuracy and timing of the tides.

4. Results of simulations with the North-Atlantic model

4.1 Introduction

The North-Atlantic model has been run from 1958 to 2002, and provides maps of the sea ice conditions for the Arctic and peripheral seas. It provides a complement to the TOPAZ and Barents Sea simulations, since the North Atlantic model has a description of the sub-grid scale features of the Arctic Sea ice cover. Where the TOPAZ model and the Barents Sea model describe the ice cover using a single ice thickness, the North Atlantic model describes the ice cover with five ice thickness categories. This makes it possible to describe the ice thickness distribution, which is important for risk assessment.

Both TOPAZ and the North Atlantic model cover the entire Arctic Ocean, but the TOPAZ system is focusing on real-time operations, which means that important historical ice information is not available from TOPAZ. The North-Atlantic model is therefore useful for the historical ice thickness information in the Arctic. In the following we will demonstrate the annual variability of the sea ice cover in the Arctic from the model, as well as a validation against observations.

4.2 Ice Thickness variability

The ice thickness can vary strongly on a year-to-year basis in the Arctic Ocean, see Figs. 14 – 17. These figures show the ice thickness at the approximate time of maximum ice extent (April) and minimum ice extent (October) for the years 1990-2001. The seasonal cycle of ice thickness results in a much thinner ice cover in October relative to April the same year. Figure 18 shows a Hovmuller (time-distance) plot for a section stretching from Greenland to the Siberian coast.

The time period from 1990 up to 1996 is a period of strong decline in the total sea ice mass in the Arctic. This can be inferred from the plots of sea ice thickness from the model as well. And even though the sea ice volume has recovered somewhat towards the mid 1990s, it remains a lot lower than in the beginning of the 1990s, up until the end of the simulations in 2002. The decline in ice thickness are also supported by observations and other model studies (Yu et al., 2004).

The mechanisms causing the decline seems to be a combination of dynamic (wind-driven) and thermodynamic effects. Based on satellite observations the export of sea ice from the Arctic to the Greenland Sea, for instance, was relatively high in the time period 1990-1996 (Kwok, 2004). Fram Strait is the section where most of the ice export from the Arctic takes place, although the export to other regions (such as the Barents sea) can be relatively high at times. However, the ice export alone is not enough to explain the decline in Arctic Sea ice volume, pointing to thermodynamical effects as well.
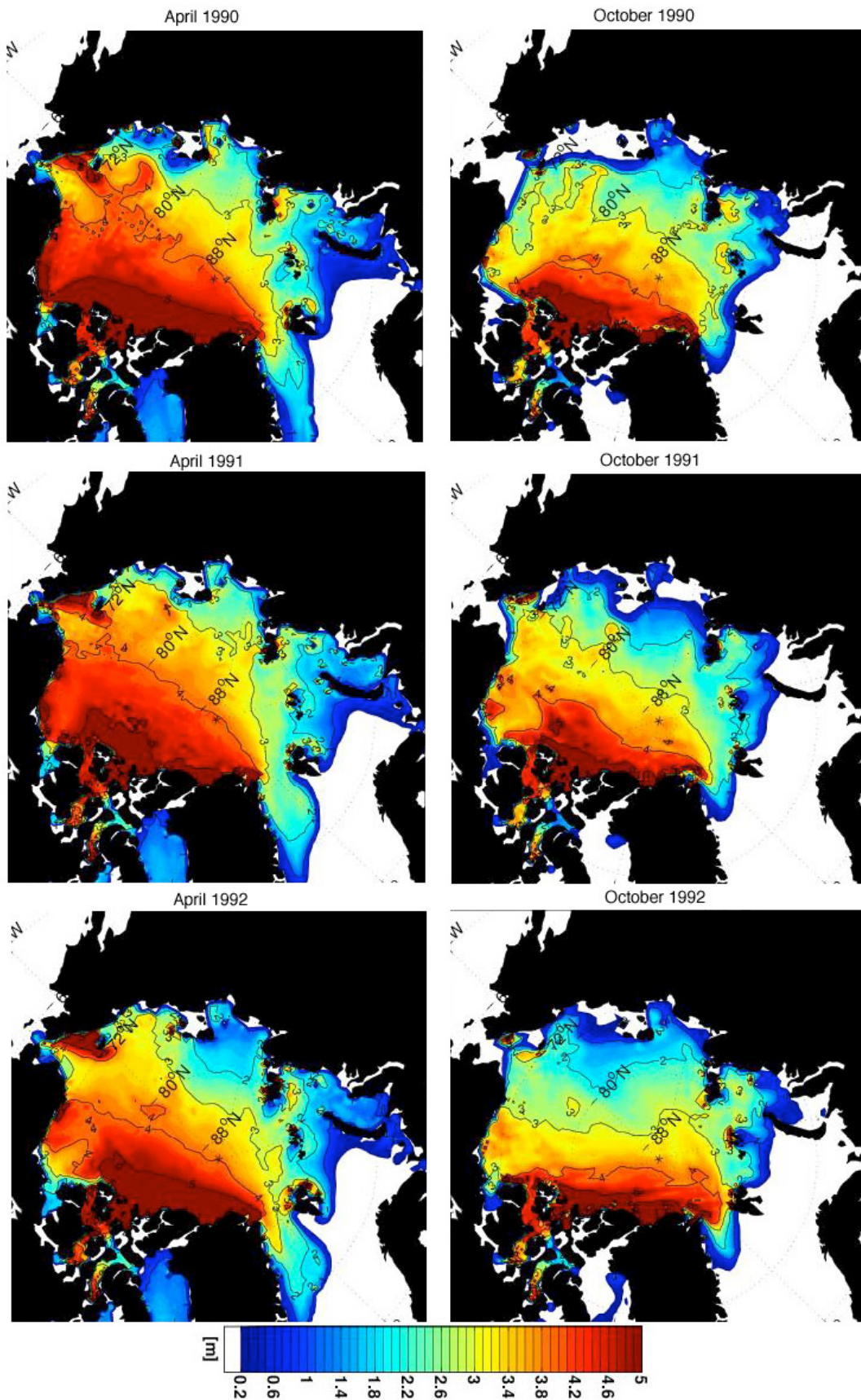
Figure 14. Ice thickness plots for months April (left) and October (right) in the years 1990-1992
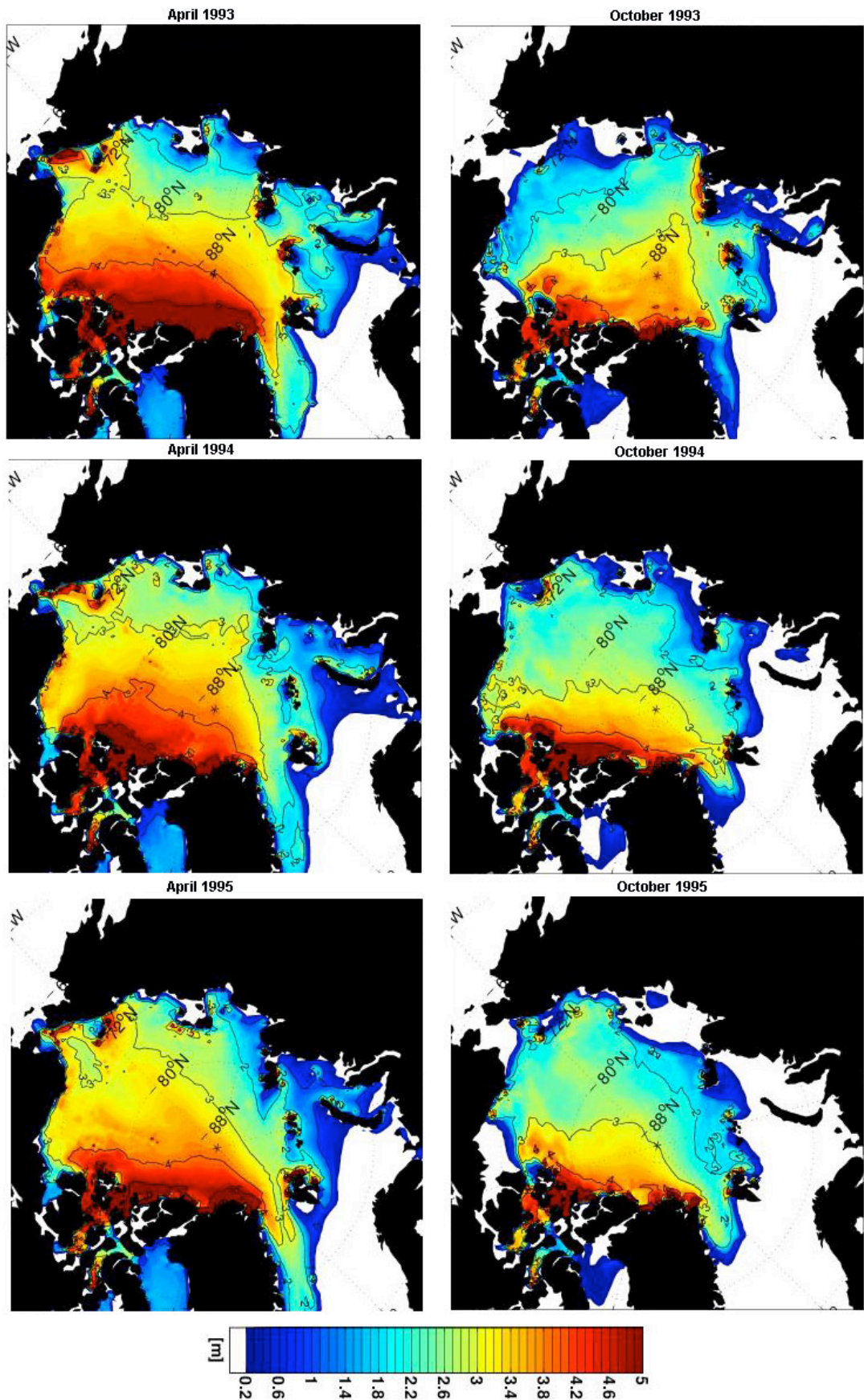
Figure 15. Ice thickness plots for months April (left) and October (right) in the years 1993 - 1995
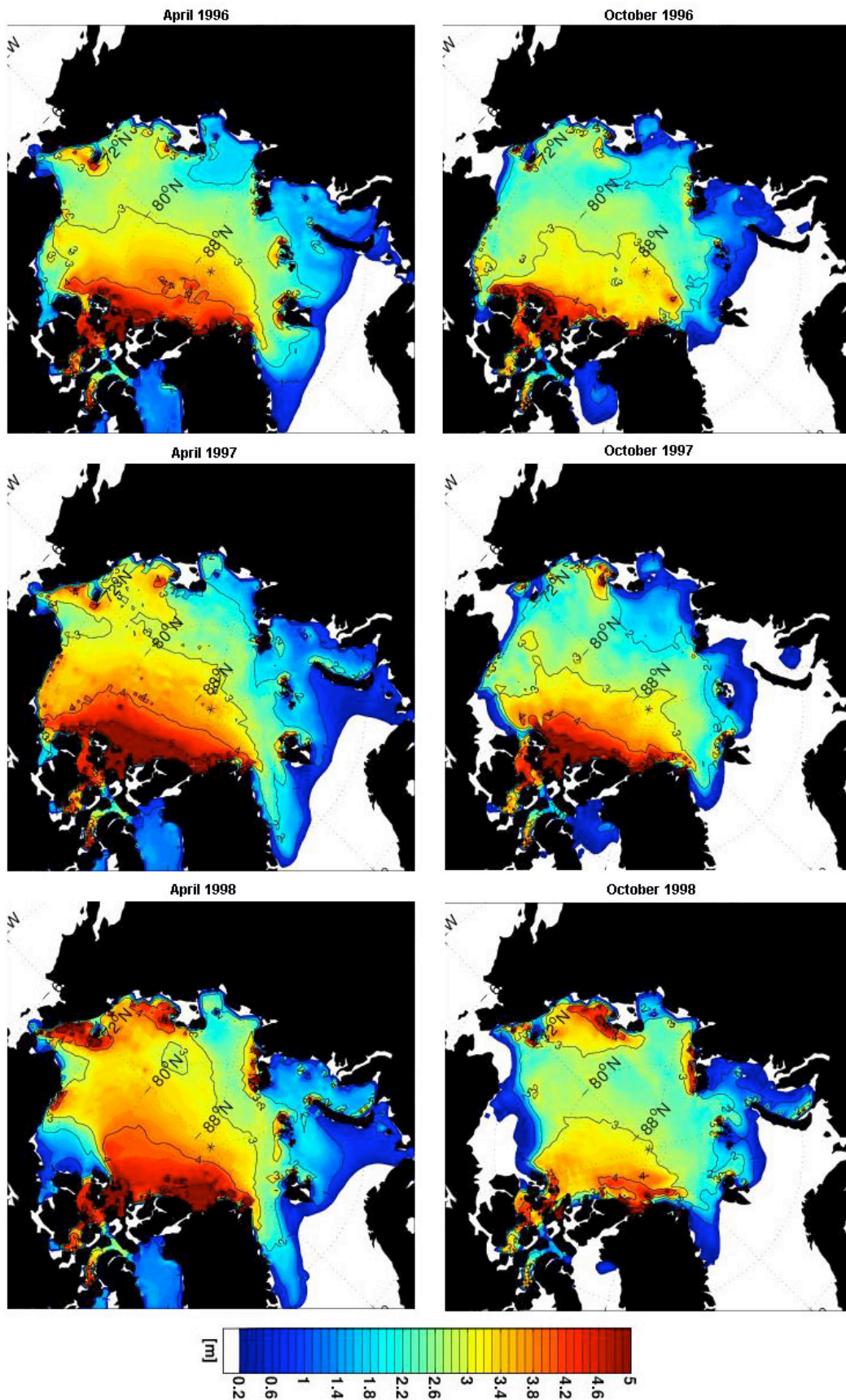
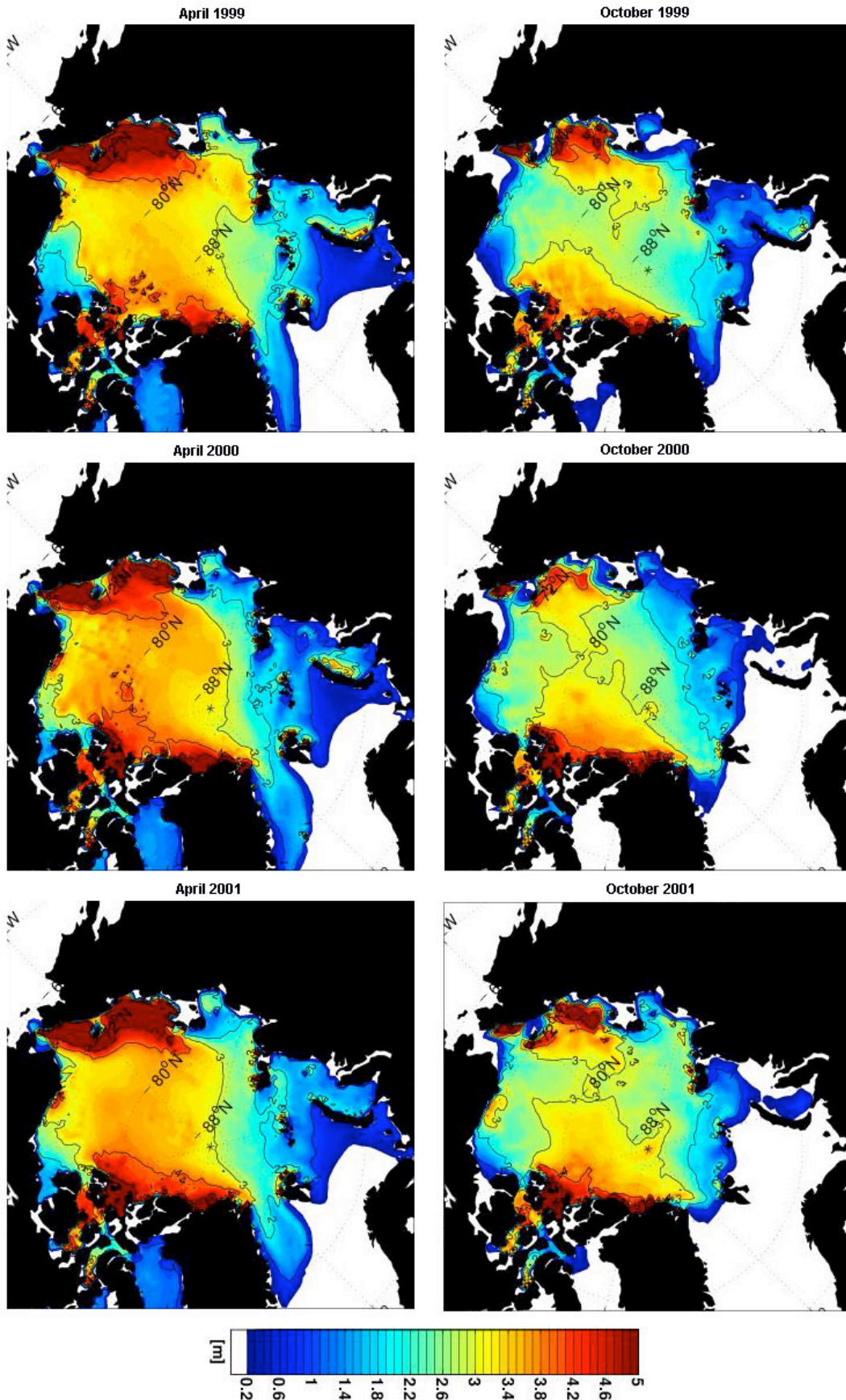*Figure 16. Ice thickness plots for months April (left) and October (right) in the years 1996-1998*

Figure 17. Ice thickness plots for months April (left) and October (right) in the years 1999-2001
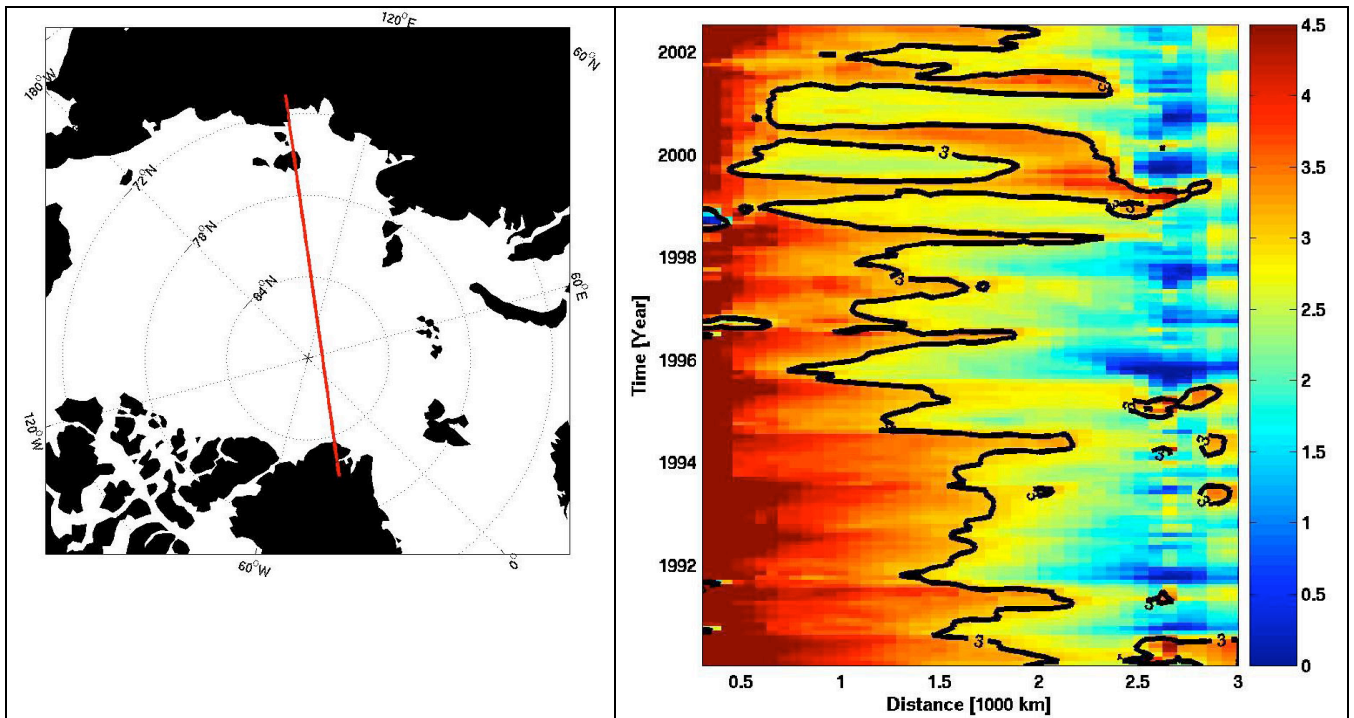
***Figure 18**. Hovmuller (time-distance) plot of ice thickness for the section on the left from Greenland to the Laptev Sea.*

4.3 Comparison between modeled and observed ice thickness

During the last decades, American and British submarines have conducted surveys in the Arctic, where they used upward-looking sonar to measure the ice draft (the amount of ice below the sea surface. Comparisons between the model and these data has been performed, showing that the model does a relatively good job of describing the sea ice draft. When viewing these comparisons, it should be remembered that the sea ice model is relatively coarse (approximately 50-80 km in the Arctic), so that the model results will tend to be much smoother than the data retrieved from the measurements (approximate resolution of 10 km).

The comparisons show that for the observations used here, stretching from 1976 to 1998, the large-scale features of the Arctic are well represented. The major discrepancy appears to be at the end of the simulation (1997-1998). However, given uncertainties in the forcing fields used to drive the sea ice model (these are generally larger for the Arctic, due to sparse data coverage), the results are show that overall the model does a good job in describing the sea ice cover.
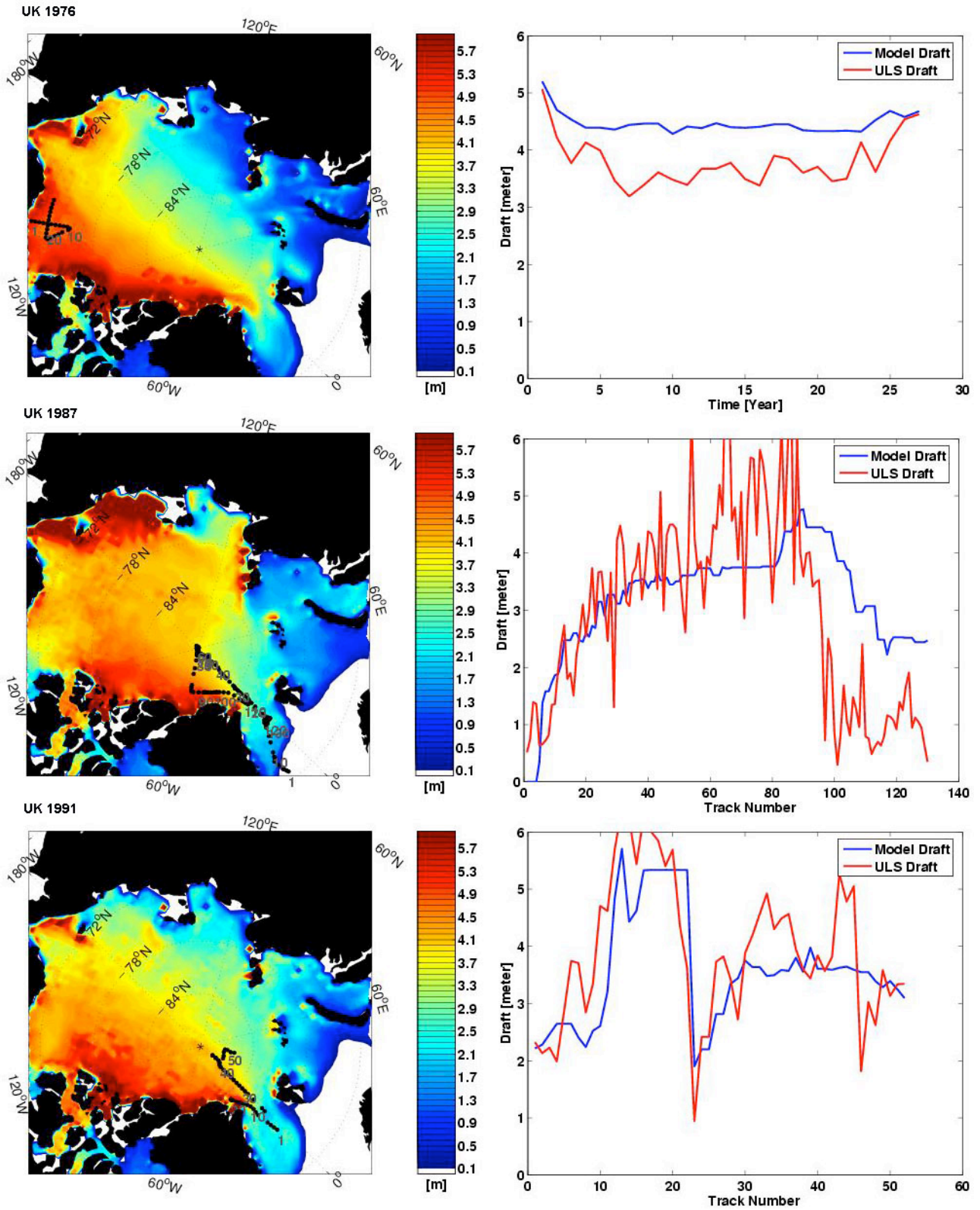
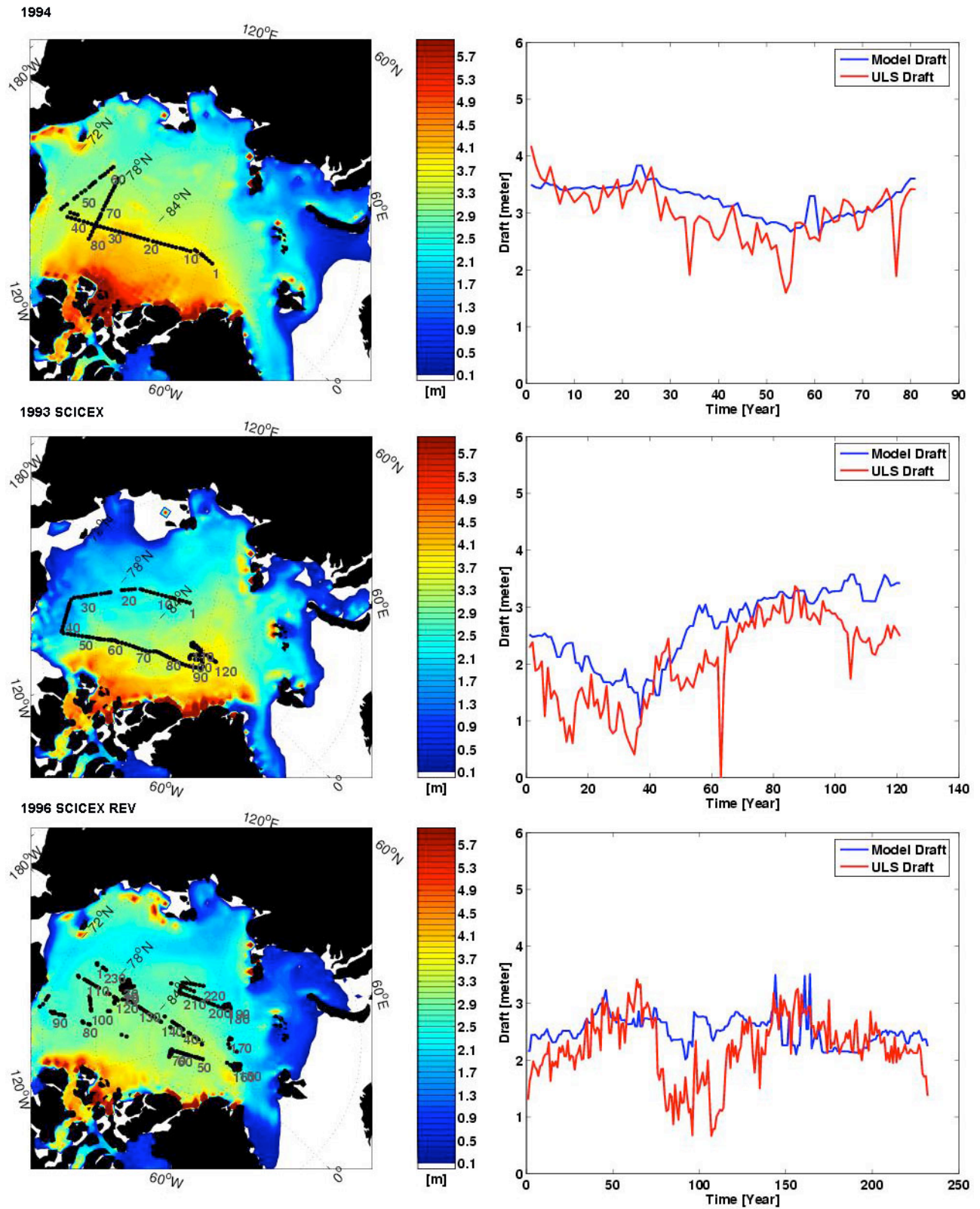*Figure 19. Comparison between ULS and model data for 1976, 1987 and 1991*

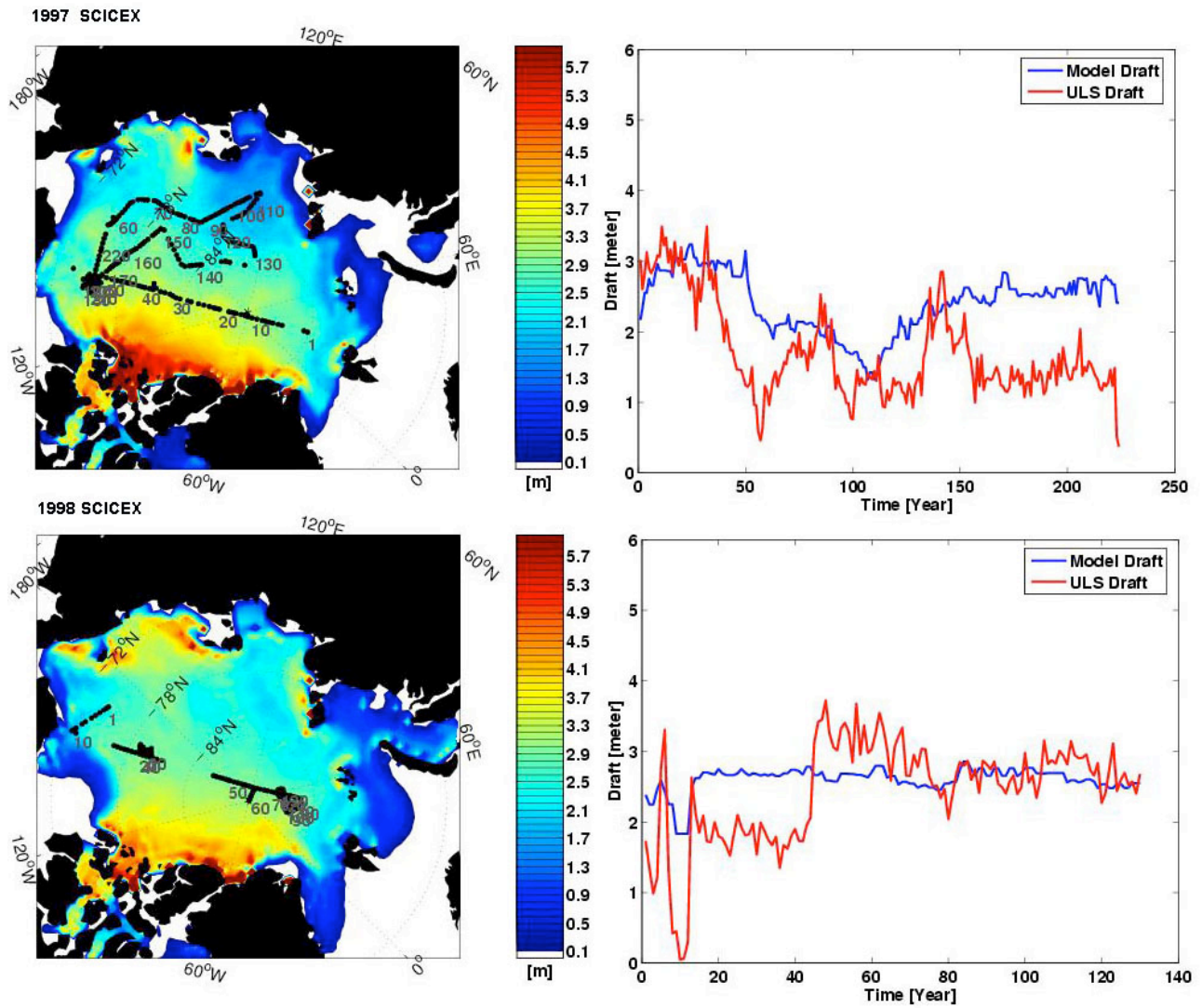*Figure 20. Comparison between model and submarine sea ice draft for 1993, 1994 and 1996*

Figure 21. Comparison between submarine and model ice draft 1997 to 1998

4.4 Monthly statistics of ice thickness in the Barents Sea

The North Atlantic model provides a much longer time series than the TOPAZ and Barents Sea model. Although the resolution is coarser than these two models, the model has shown to give a *relatively* good description of the sea ice conditions in the Barents Sea as well, specifically in the position of the Shtockman field. A comparison between the modeled and passive microwave sea ice concentration is shown in Fig. 22. The sea ice conditions in the Shtockman field vary greatly from year to year and on decadal time scales. For instance, the end of the 1970s reveal adverse sea ice conditions with very long-lasting sea ice cover. On the other hand, in the early 1990s the onset of the sea ice season was very late, and the duration of the season very short.
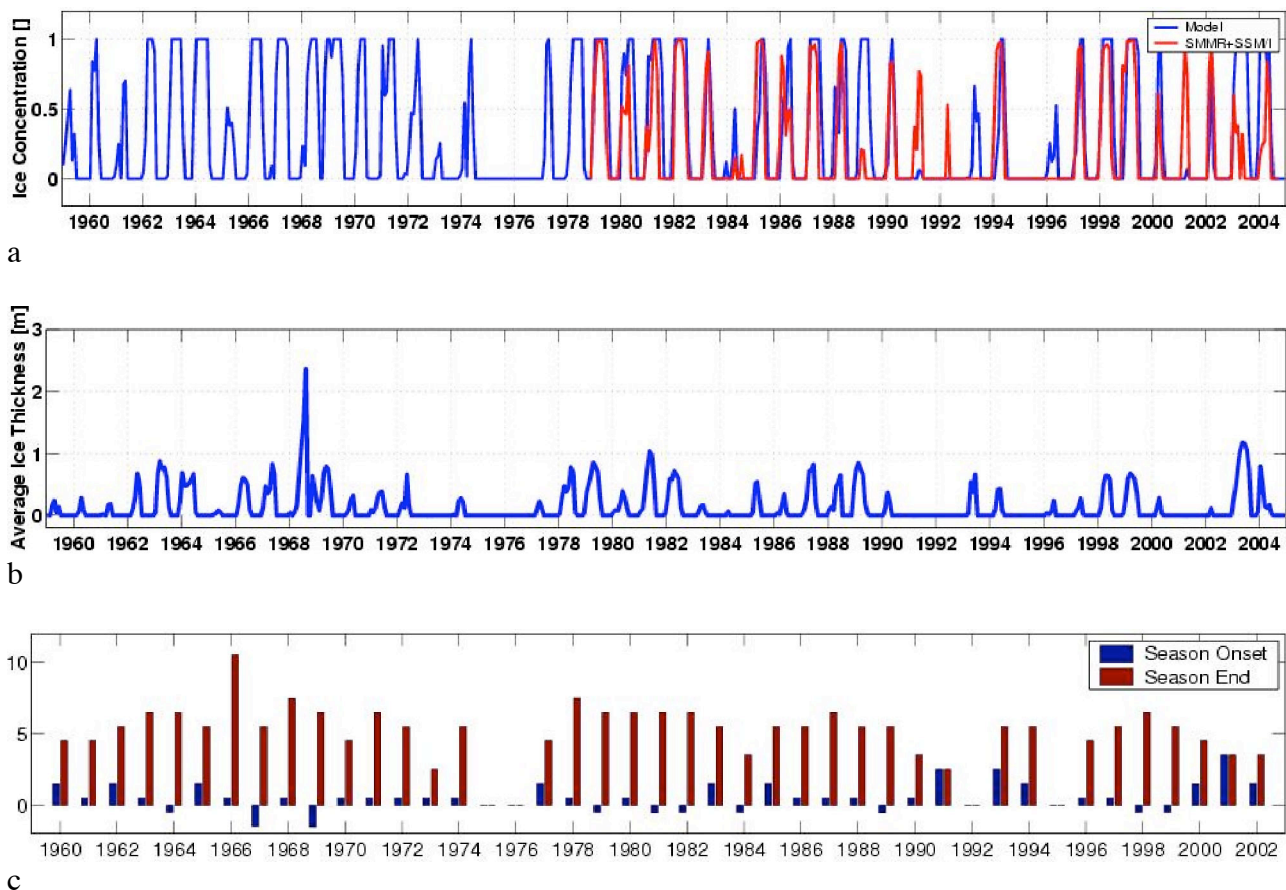
Figure 22. Sea ice concentration (a) and sea ice thickness (b) in the location of the Shtockman field. Blue is model, red is passive microwave observations. c) approximate onset and end of ice covered season at Shtockman from the model. Negative values indicate season onset the year before (Example: in 1979 the Season started in December 1978 and ended in October 1979)

In addition to the Statistics near the Shtockman field, a web-based utility has been produced which presents model data from all grid points in the Barents Sea model. The grid points are shown in Figure 23. By clicking a grid cell the user can download a csv-file (can be imported in excel) and analyze the station time series further. Examples of statistics from these data files plots are shown in Figure 24.

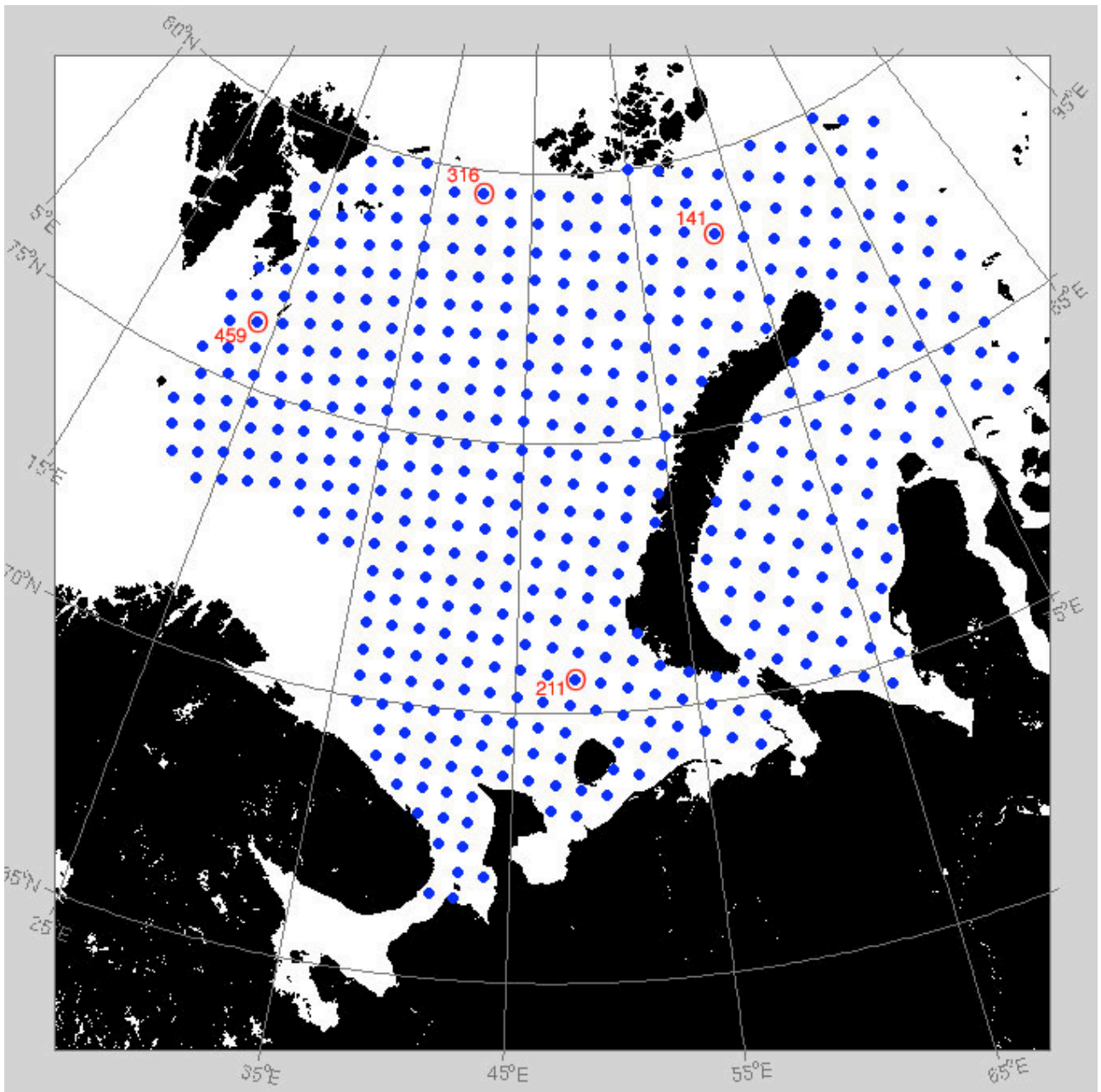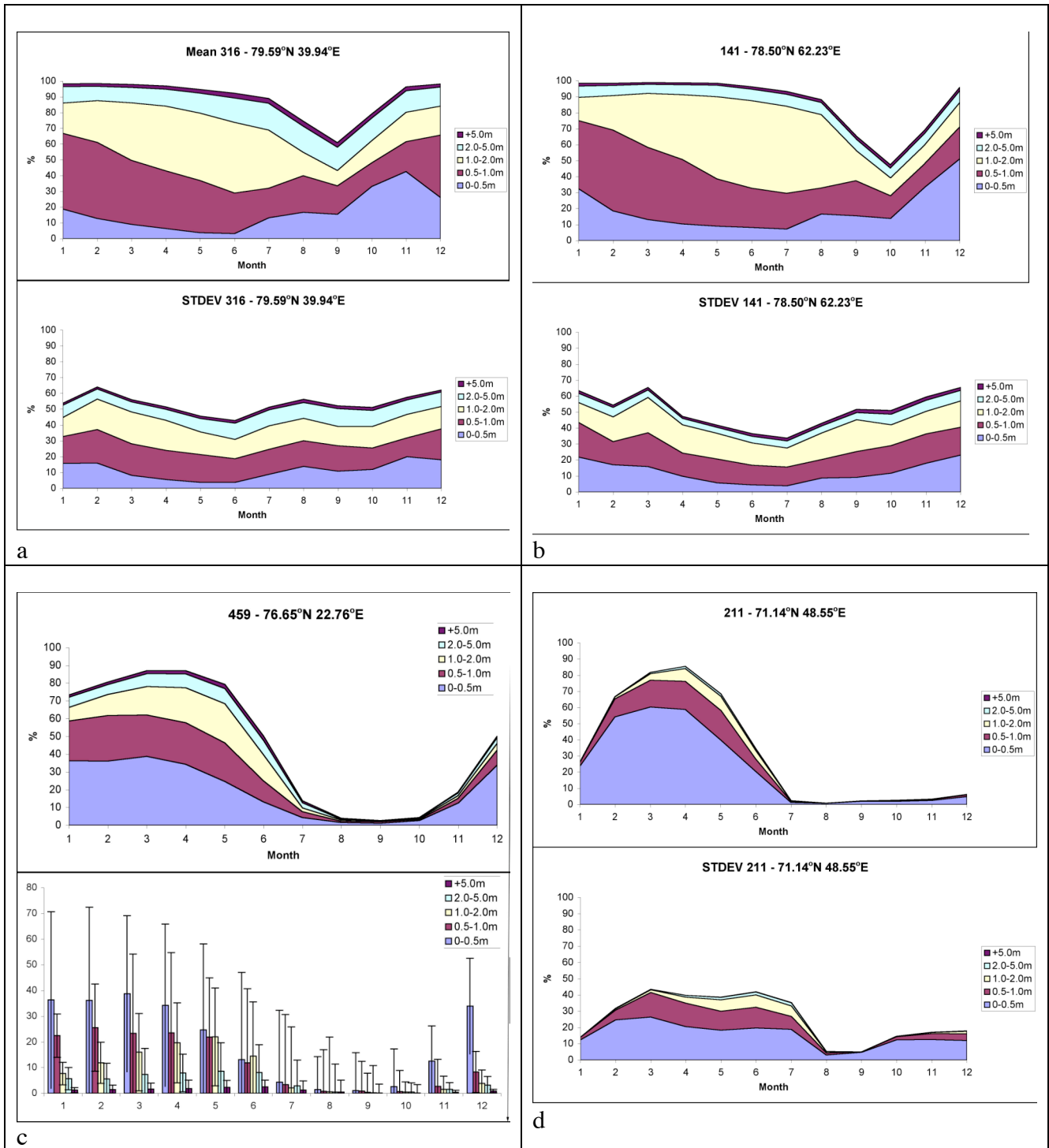***Figure 23**. Model grid cell locations for the Barents Sea*

Figure 24. *Examples of excel-statistics which can be produced from the csv-files in the web-based utility. Mean seasonal cycles and standard deviations are shown for points 141, 316, 459 and 211 in Figure 23.*

4.5 Conclusion

The North Atlantic model has been shown to give a good description of the ice conditions in the Central Arctic wrt ice thickness. The ability of the model to describe the sea ice thickness distribution makes the statistics from this model a useful tool when describing the history of sea ice thickness in the Arctic, and also in the Barents Sea. A web-based tool has been developed which makes it easy for the user to download and analyze monthly statistics from the model.

At present the model has been run in several configurations, to investigate the sensitivity of the model to using fewer or more ice thickness categories. The results from these model configurations has not been assessed for the Barents Sea, but future work should include analysis of these model setups to see if they produce better results. In addition, the historic runs should be analyzed further to reveal the transport of sea ice from the Arctic Ocean into the Barents Sea, and how this affects the sea ice cover in the Barents Sea. After all, we expect the majority of thick sea ice to be found in the Barents Sea to be transported there from the central Arctic Ocean. Local sea ice production in the Barents Sea compared to sea ice import from the Arctic is also a topic which we hope to study further.

5. The iceberg drift model

NERSC have established a collaboration with Dr. Michael Schodlok at the Alfred Wegner Institute, Bremerhaven, Germany. The iceberg group at AWI has developed a ice berg drift model, and this model has been made available for use at NERSC. The FORTRAN code has been received, but has not yet been implemented with the Barents Sea model. A brief outline of the basic equations, the model concept and results will be given along with plans for forthcoming work at NERSC.

Covering equations and parametrization

The basic equation describing iceberg motion in ice covered seas is given as

$$M \cdot d\mathbf{u} = \mathbf{F}_A + \mathbf{F}_W + \mathbf{F}_C + \mathbf{F}_{SS} + \mathbf{F}_{SI} \tag{1}$$

where M is the mass of the ice berg and u the velocity of the ice berg. The iceberg described as a point mass with finite area. The right hand side includes the forces due to air drag ($\mathbf{F}_A$), water drag ($\mathbf{F}_w$), the Coriolis force ($\mathbf{F}_c$), the slope over the sea surface ($\mathbf{F}_{ss}$) and the force due to the interaction with the sea ice cover.

The air drag and the water drag are decomposed in forces acting on the horizontal surfaces (skin drag) and on the vertical walls (form drag). The two drags can be expressed by the following expression

$$\mathbf{F}_i = \left(\tfrac{1}{2} \rho_i c_i A_{vi} + \rho_i c_{di} A_{hi} \right) \| \mathbf{v}_i - \mathbf{u} \| (\mathbf{v}_i - \mathbf{u}) \quad i = a, w \tag{2}$$

a,w stands for air and water, respectively, r_i is the medium density (air or water), c_i is the dimensionless resistance coefficient, c_{di} is the dimensionless drag coefficient for very smooth surfaces. These parameters are given empirical values in Lichey and Hellmer, and a literature survey should be made to get the most updated drag values. A_{vi} is the area of the iceberg wall facing the air/water flow, A_{hi} is the area of the horizontal iceberg surfaces in contact with the wind (top) and the ocean current (base). The $\mathbf{v}_A$ is the wind velocity obtained from wind fields from for

example NCEP/NCAR or ECMWF. The water velocity $\mathbf{v}_w$ is obtained from oceanographic circulation fields from an ocean model, by vertical integration from the sea surface down to the depth of the draft of the iceberg.

As seen in equation (1) the iceberg drift is also influenced by the Coriolis force

$$\mathbf{F}_c = 2M\Omega \sin\phi\, \mathbf{k} \times \mathbf{u}$$

where Ω (=7.27 * 10^{-5} s^{-1}) is the rotation of the earth surface, ϕ is the latitude, k is the unit vector normal to the earth surface, and $\mathbf{u}$ is the iceberg velocity. The force acting on the surface due to the slope of the sea surface is defined by

$$F_{ss} = -M\mathbf{g}\sin\alpha$$

where $\mathbf{g}$ is the acceleration due to gravity. a is the tilt of the sea surface, which is estimated from the barotropic part of the modeled ocean velocity. Sea conditions, extent and concentration, in the Barents sea is highly variable both with respect to geographical position and to season. The force due to the sea ice is in the current model split into three categories of sea ice concentration

$$F_{SI} = \begin{cases} 0 & A \leq 0 \\ \frac{1}{2}\rho_{SI} c_{SI} A_{SI} |\mathbf{v}_{si} - \mathbf{u}| (\mathbf{v}_{si} - \mathbf{u}) & 15\% < A < 90\% \\ -(\mathbf{F}_A + \mathbf{F}_W + \mathbf{F}_C + \mathbf{F}_{SS}) & A \geq 90\% \text{ and } P \geq Ps \end{cases}$$

where A(%) is the ice concentration, P (Nm^{-1}) the sea ice strength, and P_s (Nm^{-1}) is a threshold value calculated according to the formula above to make the ice resist the forces acting on the iceberg without breaking. A measure for the sea ice resistance is the sea ice strength given by the relationship

$$P = P^* h \exp\{-20(1-A)\} \text{ (Hibler, 1979)}$$

where h is the sea ice thickness pr unit area, A is the sea ice concentration. In our study the, the spatial and temporal ice thickness and concentration fields will be obtained from the ice-ocean model system the Barents Sea model. Furthermore, P* is an empirical coefficient ranging from 15000 Nm^{-2} to 30000 Nm^{-2}. In the Antarctic study performed by Lichey and Hellmer a value of 20000 Nm^{-2} was preferred. This value has to be checked up because of the large difference in ice conditions in the Weddell Sea and the Barents Sea.

The iceberg drift trajectory is calculated using an Eularian forward scheme with a given time-step, equal to 600 s in the Antarctic study with low resolution in the forcing fields. Since the Barents Sea study will be based on a much higher resolution in the ocean-ice forcing fields (4 km) one might have to decrease the time-step significantly. This has to be tested. The use of input from a high resolution, eddy resolving, to the ice drift model has not been done before at AWI, and will certainly bring new results.

The coupling of the two systems will first be done off-line; which mean that iceberg drift model will obtain forcing fields from the Barent Sea model. However, due to the very large amount of data to be dumped and stored for off-line simulations, it would be better as a second step, to incorporate the ice drift module into the model system and run it in-line with the ice-ocean model. The off-line

coupling and the test runs will create the know-how how to couple the iceberg drift module to the ice-ocean model system.

6. Conclusions and recommendation for further work

The work on sea ice modelling in 2005 has focused on setting up and testing the Barents Sea coupled ice-ocean model which is nested to the large scale TOPAZ forecasting system at NERSC. Furthermore, an iceberg drift model has been obtained from Alfred Wegener Institute, and this model will be coupled to the Barents Sea model in 2006. Then we will have a complete forecasting system for icebergs, sea ice and ocean currents including tides.

The validation of the Barents Sea model has focussed on three aspects: first a comparison of the modelled volume fluxes with observations in and out of the Barents Sea, secondly comparison of temperature and salinity fields with observations for one month in 1979, and thirdly comparison of ice extent and concentration with satellite data for four winter months in 1979. The model performs reasonably in all these comparisons, but further validation is necessary especially in the southeastern part of the Barents Sea. For iceberg drift validation, it will be specially important to validate currents and drift trajectories. Dedicated data sets for this will be required.

Other sea ice modelling results from the large-scale models an NERSC have been obtained to study regional and interannual variability of ice thickness. Comparisons have been made between modelled thickness and observed ice thickness from various submarine cruises in the Arctic basin, showing that the North Atlantic model gives fairly good estimates of the thickness. Based on this comparison, we have produced monthly ice thickness statistics for some locations in the Barents sea, including the Shtockman field, for the period 1958 to 2002. The study shows that the Shtokman field can be ice-free several winters. For example, for the month of March there has been 11 ice-free years in the last 25 years. Ice-free is then defined to be ice concentration below 30 %. When ice is present, the thickness is mainly in the 0 – 0.5 m category, but occasionally ice with thickness in the category 2.0 – 5.0 can occur.

Further work with the model development in the Barents Sea should include:

- More validation of the Barents Sea model with focus on the southeastern Barents Sea

- Implement the iceberg model as stage one model. Review the state of the art, and update the model formulation according to this. Create off line link between the iceberg model and the ice-ocean model system (Barents Sea model, ECMWF). Perform a sensitivity study by introducing a fictive ensemble of icebergs (geographic, position, size)

- Compile and analyze recent iceberg drift data to select candidate icebergs for drift simulations

- Model validation: Run new test periods with the modelling system

- Produce trajectories for the selected ice berg candidates using the Barents Sea model and ECMWF as forcing. Compare the result with observed iceberg trajectories.

- Operational use: Prepare for operational iceberg monitoring system by coupling the ice-ocean model with the iceberg drift module. Start assimilation of ice concentration into the Barents Sea model. System for updating identified icebergs to be included in the operational iceberg warning system.

- Assess the performance of the system and identify elements to be improved

7. References

Bertino (2004), Lisæter, Sagen, Counillon, Winther, Stette, Natvik, G. Evensen, Morel, Brankart, Testut, Birol, Brasseur, Verron, Schartau,, Schröter, Dombrowsky, Burillo, Gilles Larnicol, Schaeffer & Weller. Towards an Operational Prediction system for the North Atlantic and European coastal Zones – TOPAZ Final report, NERSC Technical Report, 251.

Brusdal, K., , J. Brankart, G. Halberstadt, G. Evensen, P. Brasseur, P.J. van Leeuwen, E. Dombrosky, and J. Verron. (2003). A demonstration of ensemble-based assimilation methods with a layered OGCM from the perspective of operational ocean forecasting systems, J. Marine. Sys., 40-41, 253-289.

Bleck (2002). An oceanic general circulation model framed in hybrid isopycnic-Cartesian coordinates. Ocean Modelling, Vol.4,pg 55-88.

Bleck (1992) Rooth, Hu&Smith. Salinity driven thermohaline transients in a wind- and thermohaline-forced isopycnic coordinate model of the North Atlantic. J.Phys. Oceanogr., 22, 1486-1515.

Drange (1996) and Simonsen. Formulation of air-sea fluxes in ESOP2 version of MICOM", Technical report 125, Nansen Environmental and Remote Sensing Center, Bergen, Norway

Evensen (1994). Sequential data ssimilation with a nonlinear quasi-geostropic model using Mote carlo methods to forecast error statisitics. J. Geophys. Res., 99, 10143-10162, 1994.

Evensen, (2002). Sequential data assimilation for non-linear dynamics: The ensemble Kalman filtering. In *Ocean Forecasting: Conceptual basis and applications* (eds N. Pinardi and J. D. Woods). Springer-Verlag.

Harder, M., 1996: *Dynamik, Rauhigkeit und Alter des Meereises in der Arktis - NumerischeUntersuchungenmit einemgroßkaligenModell*, Ph.D. thesis, Universität Bremen, Bremen, Germany, published by Alfred Wegener Institute: Berichte zur Polarforschung, **203**, 1996.

Hibler III (1979). A dynamic thermodynamic sea ice model. J.Phys.Oceanogr.,9, 815-845).

Hunke & Dukowicz (1997). An Elastic-Viscous-Plastic Model for Sea Ice Dynamics, Journal of Physical Oceanography), 27, pp 1849-1867.

Kwok, R. Annual cycles of multiyear sea ice coverage of the Arctic Ocean: 1999-2003. J. Geophys. Res. Vol. 109, C11004, 2004

Large, W. G., J. C. McWilliams, and S. C. Doney, Oceanic vertical mixing: A review and a model with a nonlocal boundary layer parameterization, Rev. of Geophys., 32 , 363–403, 1994.

Lisæter, K. A., Rosanova, J. and Evensen, G. (2003) "Assimilation of ice concentration into a coupled ice-ocean model, using the Ensemble Kalman Filter", *Ocean Dynamics*, 53: 368-388.

Yu, Y., G.A. Maykut, and D.A. Rothrock, "Changes in the thickness distribution of Arctic sea ice between 1958-1970 and 1993-1997," J. Geophys. Res., 109, 10.1029/2003JC001982, 2004.

Svendsen, E., K. Kloster, B. Farrelly, O. M. Johannessen, J. Johannessen, W. Campbell, P. Gloersen, D. Cavalieri and C. Matzler, 1983. Norwegian Remote Sensing Experiment: Evaluation of the Nimbus-7 SMMR for sea ice research, *J. Geophys. Res.,* 88, 2781–2791.

Zhang (2003), Thomas, Rothrock, and Lindsay, and Yu. Assimilation of ice motion observations and comparisons with submarine thickness data. J. Geophys.Res. Vol. 108, C6.